INTERNATIONAL JOURNAL FOR NUMERICAL METHODS IN ENGINEERING
Int. J. Numer. Meth. Engng 2002; **54**:1409–1430 (DOI: 10.1002/nme.470)

Anisotropic damage coupled to plasticity: Modelling based on the effective configuration concept

A. Menzel[1], M. Ekh[2,*,†], P. Steinmann[1] and K. Runesson[2]

[1] *Chair of Applied Mechanics, University of Kaiserslautern, Kaiserslautern D-67653, Germany*
[2] *Department of Solid Mechanics, Chalmers University of Technology, Göteborg SE-41296, Sweden*

SUMMARY

A model framework for anisotropic damage, that is kinetically coupled to inelastic deformations, is outlined. Key ingredients are the concept of the effective undamaged configuration and the assumption of energy equivalence. The pertinent rate equations for the chosen internal variables are integrated using the standard fully implicit scheme, and the Jacobian matrix of the resulting non-linear incremental constitutive problem is used to compute the algorithmic tangent stiffness in straightforward fashion. Numerical results showing the effect of deformation-induced anisotropy conclude the paper. Copyright © 2002 John Wiley & Sons, Ltd.

KEY WORDS: anisotropy; effective configuration; elasto-plastic damage

1. INTRODUCTION

The notion of continuum damage due to gradual disintegration on the micro-structural level is used in the macroscopic modelling of degradation of stiffness and strength of solids. The view taken by most researchers is that such damage is not a part of the deformation but is caused or rather driven by the deformation. For ductile solids, whose response is intrinsically elastic–(visco)plastic in the absence of damage, this view has lead to the conceptional notion that the evolution of damage is kinetically coupled to the evolution of inelastic deformations. Based on this view a wealth of literature has been devoted to the development of constitutive theory for damage coupled to inelastic response. In particular, we emphasize the contribution of the 'French school', References [1–5]. Other contributions are by References [6–13]. However, some researchers have preferred to introduce the concept of 'damage strain' that, besides elastic and inelastic parts, forms a part of the total strain, cf. the recent work by Armero and Oller [14].

*Correspondence to: M. Ekh, Department of Solid Mechanics, Chalmers University of Technology, Göteborg SE-41296, Sweden
†E-mail: magnus.ekh@me.chalmers.se

Received 7 May 2001
Revised 1 November 2001

Among the issues of particular concern in conjunction with establishing the appropriate constitutive framework, we mention: Admissibility from a thermodynamics viewpoint, anisotropic development of damage, micro-crack closure and possible reopening effect due to compressive stresses/strains, etc., cf. Reference [15]. In particular, as a consequence of anisotropic damage, it is inevitable that the macroscopic deformation characteristics and the current strength characteristics will also become anisotropic, and this anisotropy must be described in a rational, as well as physically realistic, fashion. To capture the anisotropy one must introduce at least a second-order internal variable, see e.g. Reference [16]. As a point of departure for the present contribution, we take the concept of an effective undamaged configuration, which is linked to the nominal damaged reference configuration via a damage deformation gradient, cf. References [17–19]. Nevertheless, in strong contrast to these classical approaches, the present damage theory, previously outlined in Steinmann and Carol [20] and further exploited in Menzel and Steinmann [21], is based on the notion of a second-order damage metric tensor and its effects on the stored strain energy. Although it is not necessary, we shall in the present contribution assume that the virgin undamaged response is isotropic. Here we shall restrict to the case of small strain theory; however, the fictitious deformation associated with damage, or rather disintegration, is truly finite and requires the kinematical framework of large strains.

The paper is organized as follows: Section 2 highlights the adopted framework of the kinetic coupling involving anisotropic damage and plasticity. In particular the concept of an effective configuration is introduced. In Section 3 we discuss the implicit integration of the obtained evolution equations. In addition, the corresponding local and global tangent operators for a Newton iteration scheme are given. A prototype model, that incorporates a Mises-type yield function, is set up in Section 4 and is used for the numerical examples in Section 5. Finally, for convenience of the reader, the Appendix summarizes essential aspects of the applied notation and reiterates useful derivatives in view of the general framework as well as the prototype model.

2. CONSTITUTIVE RELATIONS FOR TENSORIAL DAMAGE WITH KINETIC COUPLING TO PLASTICITY

2.1. Free energy and potential functions – constitutive relations

In order to restrict the formal complexity of the most general constitutive relations possible, while still adopting a realistic format of plasticity, we propose that the free energy per unit volume is decomposed into elastic and plastic parts in standard fashion as follows:

$$\Psi(\boldsymbol{\varepsilon}^{\mathrm{e}}, \boldsymbol{k}, \boldsymbol{b}) = \Psi^{\mathrm{e}}(\boldsymbol{\varepsilon}^{\mathrm{e}}, \boldsymbol{b}) + \Psi^{\mathrm{p}}(\boldsymbol{k}, \boldsymbol{b}) \tag{1}$$

where $\boldsymbol{\varepsilon}^{\mathrm{e}} = \boldsymbol{\varepsilon} - \boldsymbol{\varepsilon}^{\mathrm{p}}$ is the elastic part of the total strain $\boldsymbol{\varepsilon} = \nabla^{\mathrm{sym}}\boldsymbol{u}$, for the appropriate set up of plasticity cf. to Simo and Hughes [22] and references cited therein. We have thus introduced the following internal variables: The plastic strain $\boldsymbol{\varepsilon}^{\mathrm{p}}$, the integrity tensor $\boldsymbol{b}$, which is a contravariant second-order tensor that accounts for damage – see elaborations below, and the single hardening variable $\boldsymbol{k}$, which is chosen here as a co-variant second-order tensor. It is noted that the additive decomposition in (1) infers decoupling of the elastic and plastic characteristics.

From the Clausius–Duhem–Inequality (CDI), the following constitutive relations are obtained in standard fashion:

$$\boldsymbol{\sigma} = \frac{\partial \Psi}{\partial \boldsymbol{\varepsilon}^{\mathrm{e}}} = \frac{\partial \Psi^{\mathrm{e}}}{\partial \boldsymbol{\varepsilon}^{\mathrm{e}}}, \quad \mathscr{D} \stackrel{\mathrm{def}}{=} \boldsymbol{\sigma} : \dot{\boldsymbol{\varepsilon}}^{\mathrm{p}} + \boldsymbol{\kappa} : \dot{\boldsymbol{k}} + \boldsymbol{\beta} : \dot{\boldsymbol{b}} \geqslant 0 \tag{2}$$

where $\mathscr{D}$ denotes the rate of dissipation per unit volume. Moreover, we introduced the dissipative 'hardening stress' $\boldsymbol{\kappa}$ and the 'integrity stress' $\boldsymbol{\beta}$, that are energy-conjugated to $\boldsymbol{k}$ and $\boldsymbol{b}$, as follows:

$$\boldsymbol{\kappa} \stackrel{\mathrm{def}}{=} -\frac{\partial \Psi}{\partial \boldsymbol{k}} = -\frac{\partial \Psi^{\mathrm{p}}}{\partial \boldsymbol{k}}, \quad \boldsymbol{\beta} \stackrel{\mathrm{def}}{=} -\frac{\partial \Psi}{\partial \boldsymbol{b}} = -\left[\frac{\partial \Psi^{\mathrm{e}}}{\partial \boldsymbol{b}} + \frac{\partial \Psi^{\mathrm{p}}}{\partial \boldsymbol{b}}\right] \tag{3}$$

Next, we define the convex set $\mathbb{E}$ of plastically admissible states in the generalized stress space, i.e. the elastic domain, spanned by $\boldsymbol{\sigma}$ and $\boldsymbol{\kappa}$:

$$\mathbb{E}(\boldsymbol{b}) = \{(\boldsymbol{\sigma}, \boldsymbol{\kappa}) \mid \Phi(\boldsymbol{\sigma}, \boldsymbol{\kappa}; \boldsymbol{b}) \leqslant 0\} \tag{4}$$

where Φ is the yield function that is convex in $\boldsymbol{\sigma}$ and $\boldsymbol{\kappa}$. Moreover, in order to satisfy non-negative dissipation, it is sufficient to require that $\Phi(\mathbf{0}, \mathbf{0}; \boldsymbol{b}) < 0 \ \forall \boldsymbol{b}$.

For the formulation of the appropriate rate equations for the internal variables, we introduce the potential of Lemaitre-type

$$\Phi^*(\boldsymbol{\sigma}, \boldsymbol{\kappa}, \boldsymbol{\beta}; \boldsymbol{b}) = \Phi(\boldsymbol{\sigma}, \boldsymbol{\kappa}; \boldsymbol{b}) + \Gamma(\boldsymbol{\beta}; \boldsymbol{b}) \tag{5}$$

where Γ is the damage potential that is convex in $\boldsymbol{\beta}$. Hence, we propose for smooth Φ^* the rate equations

$$\dot{\boldsymbol{\varepsilon}}^{\mathrm{p}} = \dot{\mu} \frac{\partial \Phi^*}{\partial \boldsymbol{\sigma}} = \dot{\mu} \boldsymbol{v}_\sigma \quad \text{with } \boldsymbol{v}_\sigma \stackrel{\mathrm{def}}{=} \frac{\partial \Phi}{\partial \boldsymbol{\sigma}} \tag{6}$$

$$\dot{\boldsymbol{k}} = \dot{\mu} \frac{\partial \Phi^*}{\partial \boldsymbol{\kappa}} = \dot{\mu} \boldsymbol{v}_\kappa \quad \text{with } \boldsymbol{v}_\kappa \stackrel{\mathrm{def}}{=} \frac{\partial \Phi}{\partial \boldsymbol{\kappa}} \tag{7}$$

$$\dot{\boldsymbol{b}} = \dot{\mu} \frac{\partial \Phi^*}{\partial \boldsymbol{\beta}} = \dot{\mu} \boldsymbol{v}_\beta \quad \text{with } \boldsymbol{v}_\beta \stackrel{\mathrm{def}}{=} \frac{\partial \Gamma}{\partial \boldsymbol{\beta}} \tag{8}$$

with the corresponding Kuhn–Tucker complementary conditions

$$\dot{\mu} \geqslant 0, \quad \Phi \leqslant 0, \quad \dot{\mu} \Phi = 0 \tag{9}$$

2.2. Continuum tangent relations

Upon differentiating $(2)_1$ and $(3)_{1,2}$, we obtain (see Appendix A for notational details)

$$\begin{aligned} \dot{\boldsymbol{\sigma}} &= \mathbf{E}^{\mathrm{e}} : [\dot{\boldsymbol{\varepsilon}} - \dot{\boldsymbol{\varepsilon}}^{\mathrm{p}}] - \mathbf{D}^{\mathrm{e}} : \dot{\boldsymbol{b}} \\ \dot{\boldsymbol{\kappa}} &= -\mathbf{H} : \dot{\boldsymbol{k}} + \mathbf{Y} : \dot{\boldsymbol{b}} \\ \dot{\boldsymbol{\beta}} &= [\mathbf{D}^{\mathrm{e}}]^{\mathrm{T}} : [\dot{\boldsymbol{\varepsilon}} - \dot{\boldsymbol{\varepsilon}}^{\mathrm{p}}] + \mathbf{Y}^{\mathrm{T}} : \dot{\boldsymbol{k}} - \mathbf{G} : \dot{\boldsymbol{b}} \end{aligned} \tag{10}$$

The linearized complementary Kuhn–Tucker conditions are given in the usual fashion as

$$\dot{\mu} \geqslant 0, \quad \dot{\Phi} \leqslant 0, \quad \dot{\mu}\dot{\Phi} = 0 \tag{11}$$

Using $(10)_{1,2}$, we may express the consistency condition $\dot{\Phi} \leqslant 0$ as follows:

$$\dot{\Phi} = \dot{\Phi}^{\mathrm{tr}} - h\dot{\mu} \leqslant 0 \tag{12}$$

where $\dot{\Phi}^{\mathrm{tr}}$ is the 'trial value' of $\dot{\Phi}$ and h is the generalized plastic modulus, defined as

$$\begin{aligned} \dot{\Phi}^{\mathrm{tr}} &\stackrel{\mathrm{def}}{=} \boldsymbol{v}_\sigma : \mathbf{E}^{\mathrm{e}} : \dot{\boldsymbol{\varepsilon}} \quad \text{and} \\ h &\stackrel{\mathrm{def}}{=} \boldsymbol{v}_\sigma : [\mathbf{E}^{\mathrm{e}} : \boldsymbol{v}_\sigma + \mathbf{D}^{\mathrm{e}} : \boldsymbol{v}_\beta] + \boldsymbol{v}_\kappa : [\mathbf{H} : \boldsymbol{v}_\kappa - \mathbf{Y} : \boldsymbol{v}_\beta] - \frac{\partial \Phi}{\partial \boldsymbol{b}} : \boldsymbol{v}_\beta \end{aligned} \tag{13}$$

In the case of plastic loading (L), defined by $\dot{\Phi}^{\mathrm{tr}} > 0$, we obtain from (12) the multiplier

$$\dot{\mu} = h^{-1} \boldsymbol{v}_\sigma : \mathbf{E}^{\mathrm{e}} : \dot{\boldsymbol{\varepsilon}} > 0 \tag{14}$$

which may be inserted into $(10)_{1,2,3}$ to give, respectively,

$$\begin{aligned} \dot{\boldsymbol{\sigma}} &= \mathbf{E}^{\mathrm{ep}} : \dot{\boldsymbol{\varepsilon}}, \quad \dot{\boldsymbol{\kappa}} = \mathbf{K}^{\mathrm{ep}} : \dot{\boldsymbol{\varepsilon}}, \quad \dot{\boldsymbol{\beta}} = [\mathbf{D}^{\mathrm{ep}}]^{\mathrm{T}} : \dot{\boldsymbol{\varepsilon}} \quad \text{with} \\ \mathbf{E}^{\mathrm{ep}} &= \mathbf{E}^{\mathrm{e}} - h^{-1} [\mathbf{E}^{\mathrm{e}} : \boldsymbol{v}_\sigma + \mathbf{D}^{\mathrm{e}} : \boldsymbol{v}_\beta] \otimes [\boldsymbol{v}_\sigma : \mathbf{E}^{\mathrm{e}}] \\ \mathbf{K}^{\mathrm{ep}} &= -h^{-1} [\mathbf{H} : \boldsymbol{v}_\kappa - \mathbf{Y} : \boldsymbol{v}_\beta] \otimes [\boldsymbol{v}_\sigma : \mathbf{E}^{\mathrm{e}}] \\ [\mathbf{D}^{\mathrm{ep}}]^{\mathrm{T}} &= [\mathbf{D}^{\mathrm{e}}]^{\mathrm{T}} - h^{-1} [[\mathbf{D}^{\mathrm{e}}]^{\mathrm{T}} : \boldsymbol{v}_\sigma - \mathbf{Y} : \boldsymbol{v}_\kappa + \mathbf{G} : \boldsymbol{v}_\beta] \otimes [\boldsymbol{v}_\sigma : \mathbf{E}^{\mathrm{e}}] \end{aligned} \tag{15}$$

Note that $\mathbf{E}^{\mathrm{ep}}$, $\mathbf{K}^{\mathrm{ep}}$ and $[\mathbf{D}^{\mathrm{ep}}]^{\mathrm{T}}$ do in general not possess major symmetry due to the non-associated evolution equation (8). Next, in the case of elastic unloading (U), defined by $\dot{\Phi}^{\mathrm{tr}} \leqslant 0$, we obtain $\dot{\mu} = 0$ and it follows trivially from $(10)_{1,2,3}$ that

$$\dot{\boldsymbol{\sigma}} = \mathbf{E}^{\mathrm{e}} : \dot{\boldsymbol{\varepsilon}}, \quad \dot{\boldsymbol{\kappa}} = \mathbf{0} \quad \text{and} \quad \dot{\boldsymbol{\beta}} = [\mathbf{D}^{\mathrm{e}}]^{\mathrm{T}} : \dot{\boldsymbol{\varepsilon}} \tag{16}$$

Since $\boldsymbol{b}$ is constant at unloading, it appears that $(16)_1$ is a secant relation that represents a degraded elastic response. Hence, in the case of linear elastic response, then $\mathbf{E}^{\mathrm{e}}$ is a constant tensor at unloading. Moreover the integrity stress changes even upon unloading due to the dependence on $\mathbf{E}^{\mathrm{e}}$ in (3).

2.3. The effective configuration concept

In the sequel we give the rationale for introducing the integrity $\boldsymbol{b}$, whereby we shall adopt the view of Steinmann and Carol [20] and introduce the effective configuration which refers to the undamaged state. However, we emphasize that all balance equations are established with respect to the nominal configuration $\mathscr{B}$, which relates to the damaged state.

It is noted that the effective configuration is incompatible similarly to the so-called intermediate configuration in the context of the multiplicative decomposition for large strain in-elasticity. The corresponding linear tangent map, which maps elements of the effective tangent space $T\bar{\mathscr{B}}$ to elements of the nominal tangent space $T\mathscr{B}$, is denoted by $\bar{\boldsymbol{F}}$ and can be interpreted as the damage deformation gradient. Hence, $\bar{\boldsymbol{F}}$ carries information about the reduced integrity of $\mathscr{B}$ as compared to the effective space. Although the actual deformation

from $\mathscr{B}$ is assumed to be small in this paper, the reduction of integrity is truly finite, since $\bar{\boldsymbol{F}} \cdot \bar{\boldsymbol{I}} \cdot \bar{\boldsymbol{F}}^{\mathrm{t}} \in [\boldsymbol{I}, \boldsymbol{0}]$, see Remark 2.2.

Next, we may use $\bar{\boldsymbol{F}}$ to perform standard pull-back and push-forward operations. Thus, the effective strain tensor $\bar{\boldsymbol{\varepsilon}}$, which we consider to be of co-variant nature, is obtained from the nominal strain $\boldsymbol{\varepsilon}$ via the co-variant pull-back

$$\bar{\boldsymbol{\varepsilon}} = \bar{\boldsymbol{F}}^{\mathrm{t}} \cdot \boldsymbol{\varepsilon} \cdot \bar{\boldsymbol{F}} \tag{17}$$

Moreover, we introduce the symmetric second-order tensor $\bar{\boldsymbol{b}}$, which we consider to be of contra-variant nature, to represent the full integrity with respect to the effective configuration. The reduced integrity $\boldsymbol{b}$ in $\mathscr{B}$ is obtained via the contra-variant push-forward

$$\boldsymbol{b} = \bar{\boldsymbol{F}} \cdot \bar{\boldsymbol{b}} \cdot \bar{\boldsymbol{F}}^{\mathrm{t}} \tag{18}$$

Accordingly, the effective stress tensor $\bar{\boldsymbol{\sigma}}$, which we consider to be of contra-variant nature, is obtained from the nominal stress tensor $\boldsymbol{\sigma}$ via the contra-variant pull-back

$$\bar{\boldsymbol{\sigma}} = \bar{\boldsymbol{F}}^{-1} \cdot \boldsymbol{\sigma} \cdot \bar{\boldsymbol{F}}^{-\mathrm{t}} \tag{19}$$

The essential idea for damage evolution will be that the eigenvalues of $\boldsymbol{b}$ reduce down to zero, which corresponds to a state of complete degradation or rather disintegration.

In the sequel we assume $\bar{\boldsymbol{b}}$ to coincide with the identity tensor $\bar{\boldsymbol{I}}$ in $T\bar{\mathscr{B}}$, hence $\bar{\boldsymbol{b}} \overset{\text{def}}{=} \bar{\boldsymbol{I}}$. It is thus implicit that $\boldsymbol{b} \overset{\text{def}}{=} \bar{\boldsymbol{F}} \cdot \bar{\boldsymbol{I}} \cdot \bar{\boldsymbol{F}}^{\mathrm{t}}$ is a symmetric, positive definite tensor as long as the degradation has not been completed. Since $\bar{\boldsymbol{F}}$ is initially equal to the identity mapping, this results in $\boldsymbol{b} = \boldsymbol{I}$ as long as no damage evolution has taken place. However, it would be possible to let a non-spherical value of $\bar{\boldsymbol{b}}$ – or a non-spherical initial $\bar{\boldsymbol{F}}$ – represent restricted forms of initial anisotropy; thereby avoiding the classical use of a separate set of structural tensors; cf. Reference [23].

2.4. Postulate of strain energy equivalence

In order to define Ψ^{e} and Ψ^{p} explicitly, we adopt the concept of strain energy equivalence between the states in the effective and nominal settings, cf. Reference [2], i.e.

$$\Psi^{\mathrm{e}}(\boldsymbol{\varepsilon}^{\mathrm{e}}, \boldsymbol{b}) \overset{\text{def}}{=} \bar{\Psi}^{\mathrm{e}}(\bar{\boldsymbol{\varepsilon}}^{\mathrm{e}}, \bar{\boldsymbol{b}}), \quad \Psi^{\mathrm{p}}(\boldsymbol{k}, \boldsymbol{b}) \overset{\text{def}}{=} \bar{\Psi}^{\mathrm{p}}(\bar{\boldsymbol{k}}, \bar{\boldsymbol{b}}) \tag{20}$$

where $\bar{\Psi}^{\mathrm{e}}$ and $\bar{\Psi}^{\mathrm{p}}$ are the energy functions that represent the virgin isotropic response in the effective configuration.

As to the explicit definition of $\bar{\Psi}^{\mathrm{e}}(\bar{\boldsymbol{\varepsilon}}^{\mathrm{e}}, \bar{\boldsymbol{b}})$, we first note that $\bar{\boldsymbol{\varepsilon}}^{\mathrm{e}}$ and $\bar{\boldsymbol{b}}$ are mappings of $\boldsymbol{\varepsilon}^{\mathrm{e}}$ and $\boldsymbol{b}$ as defined by (17) and (18). It is convenient to introduce mixed invariants of $\bar{\boldsymbol{\varepsilon}}^{\mathrm{e}}$ and $\bar{\boldsymbol{b}} \overset{\text{def}}{=} \bar{\boldsymbol{I}}$ as arguments of $\bar{\Psi}^{\mathrm{e}}$:

$$\begin{aligned}
i_1^{(\bar{\varepsilon}^{\mathrm{e}})} &\overset{\text{def}}{=} \bar{\boldsymbol{I}} : \bar{\boldsymbol{\varepsilon}}^{\mathrm{e}} = \bar{\boldsymbol{b}} : \bar{\boldsymbol{\varepsilon}}^{\mathrm{e}} = \boldsymbol{b} : \boldsymbol{\varepsilon}^{\mathrm{e}} \\
i_2^{(\bar{\varepsilon}^{\mathrm{e}})} &\overset{\text{def}}{=} \bar{\boldsymbol{I}} : [\bar{\boldsymbol{\varepsilon}}^{\mathrm{e}}]^2 = \bar{\boldsymbol{b}} : [\bar{\boldsymbol{\varepsilon}}^{\mathrm{e}} \cdot \bar{\boldsymbol{b}} \cdot \bar{\boldsymbol{\varepsilon}}^{\mathrm{e}}] = \boldsymbol{b} : [\boldsymbol{\varepsilon}^{\mathrm{e}} \cdot \boldsymbol{b} \cdot \boldsymbol{\varepsilon}^{\mathrm{e}}] \\
i_3^{(\bar{\varepsilon}^{\mathrm{e}})} &\overset{\text{def}}{=} \bar{\boldsymbol{I}} : [\bar{\boldsymbol{\varepsilon}}^{\mathrm{e}}]^3 = \bar{\boldsymbol{b}} : [\bar{\boldsymbol{\varepsilon}}^{\mathrm{e}} \cdot \bar{\boldsymbol{b}} \cdot \bar{\boldsymbol{\varepsilon}}^{\mathrm{e}} \cdot \bar{\boldsymbol{b}} \cdot \bar{\boldsymbol{\varepsilon}}^{\mathrm{e}}] = \boldsymbol{b} : [\boldsymbol{\varepsilon}^{\mathrm{e}} \cdot \boldsymbol{b} \cdot \boldsymbol{\varepsilon}^{\mathrm{e}} \cdot \boldsymbol{b} \cdot \boldsymbol{\varepsilon}^{\mathrm{e}}]
\end{aligned} \tag{21}$$

whereby the mappings (17) and (18) have been applied in order to compute $i_{1,2,3}^{(\bar{\varepsilon}^{\mathrm{e}})}$ in terms of the nominal arguments $\boldsymbol{\varepsilon}^{\mathrm{e}}$ and $\boldsymbol{b}$. Clearly, in the special case of isotropic damage, defined by $\boldsymbol{b}=b\boldsymbol{I}$ with $b\leqslant 1$ a scalar measure of the integrity, we obtain

$$i_l^{(\bar{\varepsilon}^{\mathrm{e}})}=b^l i_l^{(\varepsilon^{\mathrm{e}})} \quad \text{with } i_l^{(\varepsilon^{\mathrm{e}})} \stackrel{\text{def}}{=} \boldsymbol{I}:[\boldsymbol{\varepsilon}^{\mathrm{e}}]^l; \quad l=1,2,3 \tag{22}$$

For the proper definition of $\bar{\Psi}^{\mathrm{p}}(\bar{\boldsymbol{k}},\bar{\boldsymbol{b}})$, we shall directly choose the classical format of isotropic hardening. It is then sufficient to introduce the first invariant of the effective variable

$$i_1^{(\bar{k})} \stackrel{\text{def}}{=} \bar{\boldsymbol{I}}:\bar{\boldsymbol{k}}=\boldsymbol{b}:\boldsymbol{k} \stackrel{\text{def}}{=} \bar{k} \tag{23}$$

as the appropriate argument of $\bar{\Psi}^{\mathrm{p}}$. Summarizing, we then rewrite the free energy in (1) as

$$\Psi(\boldsymbol{\varepsilon}^{\mathrm{e}},\boldsymbol{k},\boldsymbol{b})=\bar{\Psi}^{\mathrm{e}}(i_1^{(\bar{\varepsilon}^{\mathrm{e}})},i_2^{(\bar{\varepsilon}^{\mathrm{e}})},i_3^{(\bar{\varepsilon}^{\mathrm{e}})})+\bar{\Psi}^{\mathrm{p}}(\bar{k}) \tag{24}$$

from which $\boldsymbol{\sigma}$, $\boldsymbol{\kappa}$ and $\boldsymbol{\beta}$ can be derived. However, we shall postpone the detailed execution of this exercise until Section 4, where we choose a prototype model.

Remark 2.1
Conceptually, the internal variable $\bar{k}$ pertinent to the effective configuration accounts for isotropic hardening of the undamaged material, whereas the corresponding conjugate force in the nominal setting accounts for anisotropic effects. Moreover, upon introducing the second and third invariant $i_2^{(\bar{k})}$ and $i_3^{(\bar{k})}$ into the plastic part of the free energy function Ψ^{p}, we would be able to incorporate kinematic hardening in the model framework.

A natural consequence of the strain energy equivalence postulate is the following choice of representation of the yield function Φ:

$$\Phi(\boldsymbol{\sigma},\boldsymbol{\kappa};\boldsymbol{b}) \stackrel{\text{def}}{=} \bar{\Phi}(\bar{\boldsymbol{\sigma}},\bar{\boldsymbol{\kappa}};\bar{\boldsymbol{b}}) \stackrel{\text{def}}{=} \bar{\Phi}\,(i_1^{(\bar{\sigma})},i_2^{(\bar{\sigma})},i_3^{(\bar{\sigma})},i_1^{(\bar{\kappa})}) \tag{25}$$

where we introduced the mixed invariants

$$\begin{aligned}
i_1^{(\bar{\sigma})} &\stackrel{\text{def}}{=} \bar{\boldsymbol{I}}:\bar{\boldsymbol{\sigma}}=\bar{\boldsymbol{b}}^{-1}:\bar{\boldsymbol{\sigma}}=\boldsymbol{b}^{-1}:\boldsymbol{\sigma} \\
i_2^{(\bar{\sigma})} &\stackrel{\text{def}}{=} \bar{\boldsymbol{I}}:[\bar{\boldsymbol{\sigma}}]^2=\bar{\boldsymbol{b}}^{-1}:[\bar{\boldsymbol{\sigma}}\cdot\bar{\boldsymbol{b}}^{-1}\cdot\bar{\boldsymbol{\sigma}}]=\boldsymbol{b}^{-1}:[\boldsymbol{\sigma}\cdot\boldsymbol{b}^{-1}\cdot\boldsymbol{\sigma}] \\
i_3^{(\bar{\sigma})} &\stackrel{\text{def}}{=} \bar{\boldsymbol{I}}:[\bar{\boldsymbol{\sigma}}]^3=\bar{\boldsymbol{b}}^{-1}:[\bar{\boldsymbol{\sigma}}\cdot\bar{\boldsymbol{b}}^{-1}\cdot\bar{\boldsymbol{\sigma}}\cdot\bar{\boldsymbol{b}}^{-1}\cdot\bar{\boldsymbol{\sigma}}]=\boldsymbol{b}^{-1}:[\boldsymbol{\sigma}\cdot\boldsymbol{b}^{-1}\cdot\boldsymbol{\sigma}\cdot\boldsymbol{b}^{-1}\cdot\boldsymbol{\sigma}]
\end{aligned} \tag{26}$$

and the first invariant of the effective hardening stress

$$i_1^{(\bar{\kappa})} \stackrel{\text{def}}{=} \bar{\boldsymbol{I}}:\bar{\boldsymbol{\kappa}}=\boldsymbol{b}^{-1}:\boldsymbol{\kappa} \stackrel{\text{def}}{=} 3\bar{\kappa} \tag{27}$$

The representation in (25) may be interpreted as the *effective stress postulate* which is known in the literature, since it infers that the nominal stresses are replaced by the corresponding effective counterparts as the arguments of $\bar{\Phi}$ that is valid for the undamaged response.

Finally, a suitable representation of Γ in the damage potential is

$$\Gamma(\boldsymbol{\beta};\boldsymbol{b}) \stackrel{\text{def}}{=} \bar{\Gamma}(\bar{\boldsymbol{\beta}};\bar{\boldsymbol{b}}^{-1}) \stackrel{\text{def}}{=} \bar{\Gamma}(i_1^{(\bar{\beta})}, i_2^{(\bar{\beta})}, i_3^{(\bar{\beta})}) \tag{28}$$

where the mixed invariants of the integrity stress follow as

$$\begin{aligned} i_1^{(\bar{\beta})} &\stackrel{\text{def}}{=} \bar{\boldsymbol{I}} : \bar{\boldsymbol{\beta}} = \bar{\boldsymbol{b}} : \bar{\boldsymbol{\beta}} = \boldsymbol{b} : \boldsymbol{\beta} \\ i_2^{(\bar{\beta})} &\stackrel{\text{def}}{=} \bar{\boldsymbol{I}} : [\bar{\boldsymbol{\beta}}]^2 = \bar{\boldsymbol{b}} : [\bar{\boldsymbol{\beta}} \cdot \bar{\boldsymbol{b}} \cdot \bar{\boldsymbol{\beta}}] = \boldsymbol{b} : [\boldsymbol{\beta} \cdot \boldsymbol{b} \cdot \boldsymbol{\beta}] \\ i_3^{(\bar{\beta})} &\stackrel{\text{def}}{=} \bar{\boldsymbol{I}} : [\bar{\boldsymbol{\beta}}]^3 = \bar{\boldsymbol{b}} : [\bar{\boldsymbol{\beta}} \cdot \bar{\boldsymbol{b}} \cdot \bar{\boldsymbol{\beta}} \cdot \bar{\boldsymbol{b}} \cdot \bar{\boldsymbol{\beta}}] = \boldsymbol{b} : [\boldsymbol{\beta} \cdot \boldsymbol{b} \cdot \boldsymbol{\beta} \cdot \boldsymbol{b} \cdot \boldsymbol{\beta}] \end{aligned} \tag{29}$$

We remark that the concepts of effective stress and effective strain, which are typically applied in continuum damage mechanics, are in some sense a natural outcome of the proposed framework based on the concepts of effective configuration and strain energy equivalence. Moreover, both the nominal and effective stress tensors are always symmetric within this thermodynamically consistent formulation which is, in contrast to many other proposals, concerned with second-order damage.

Finally in this subsection, we remark that in practice it may be necessary to violate the restrictive formulation in (28) by choosing the most suitable expression for $\Gamma(\boldsymbol{\beta}, \boldsymbol{b})$. An example of such a choice is given in conjunction with the description of the prototype model in Section 4.

Remark 2.2
It appears from the transformations in (27) and (29) that $\boldsymbol{\kappa}$ is considered as a contra-variant variable, whereas $\boldsymbol{\beta}$ is considered as a co-variant variable. Even though this distinction is usually not necessary in the geometrically linear setting its benefits will become apparent later.

3. CONSTITUTIVE INTEGRATOR

We recall the constitutive rate equations in the following form:

$$\begin{aligned} \dot{\boldsymbol{\varepsilon}}^{\mathrm{e}} &= \dot{\boldsymbol{\varepsilon}} - \dot{\mu}\boldsymbol{v}_{\sigma}(\boldsymbol{\sigma}(\boldsymbol{\varepsilon}^{\mathrm{e}}, \boldsymbol{b}), \boldsymbol{\kappa}(\boldsymbol{k}, \boldsymbol{b}); \boldsymbol{b}) \\ \dot{\boldsymbol{k}} &= \dot{\mu}\boldsymbol{v}_{\kappa}(\boldsymbol{\sigma}(\boldsymbol{\varepsilon}^{\mathrm{e}}, \boldsymbol{b}), \boldsymbol{\kappa}(\boldsymbol{k}, \boldsymbol{b}); \boldsymbol{b}) \\ \dot{\boldsymbol{b}} &= \dot{\mu}\boldsymbol{v}_{\beta}(\boldsymbol{\beta}(\boldsymbol{\varepsilon}^{\mathrm{e}}, \boldsymbol{k}, \boldsymbol{b}); \boldsymbol{b}) \end{aligned} \tag{30}$$

together with the Kuhn–Tucker conditions

$$\dot{\mu} \geqslant 0\,, \quad \Phi(\boldsymbol{\sigma}(\boldsymbol{\varepsilon}^{\mathrm{e}}, \boldsymbol{b}), \boldsymbol{\kappa}(\boldsymbol{k}, \boldsymbol{b}); \boldsymbol{b}) \leqslant 0, \quad \dot{\mu}\Phi(\boldsymbol{\sigma}(\boldsymbol{\varepsilon}^{\mathrm{e}}, \boldsymbol{b}), \boldsymbol{\kappa}(\boldsymbol{k}, \boldsymbol{b}); \boldsymbol{b}) = 0 \tag{31}$$

where the generic constitutive relations for the functions $\boldsymbol{\sigma}(\boldsymbol{\varepsilon}^{\mathrm{e}}, \boldsymbol{b})$, $\boldsymbol{\kappa}(\boldsymbol{k}, \boldsymbol{b})$ and $\boldsymbol{\beta}(\boldsymbol{\varepsilon}^{\mathrm{e}}, \boldsymbol{k}, \boldsymbol{b})$ are given in (2) and (3), respectively.

Next, consider a partition $0 = t_0 < \cdots < t_n < t_{n+1} < \cdots < t_N = T$ of the time interval of interest $\mathbb{T} = [0, T]$. Applying the backward Euler rule to the set of relations (30)–(31), while

using the notation $\boldsymbol{\varepsilon}^{\mathrm{e}}_n = \boldsymbol{\varepsilon}^{\mathrm{e}}(t_n)$ for the approximate value of $\boldsymbol{\varepsilon}^{\mathrm{e}}$ at time t_n and for simplicity the abbreviation $\boldsymbol{\varepsilon}^{\mathrm{e}} \stackrel{\mathrm{def}}{=} \boldsymbol{\varepsilon}^{\mathrm{e}}_{n+1}$, we obtain the algorithmic counterpart of (30)

$$\begin{aligned} \boldsymbol{\varepsilon}^{\mathrm{e}} &= \boldsymbol{\varepsilon}^{\mathrm{e,tr}} - \Delta\mu\, \boldsymbol{v}_\sigma(\boldsymbol{\sigma}(\boldsymbol{\varepsilon}^{\mathrm{e}}, \boldsymbol{b}), \boldsymbol{\kappa}(\boldsymbol{k}, \boldsymbol{b}); \boldsymbol{b}) \\ \boldsymbol{k} &= \boldsymbol{k}_n + \Delta\mu\, \boldsymbol{v}_\kappa(\boldsymbol{\sigma}(\boldsymbol{\varepsilon}^{\mathrm{e}}, \boldsymbol{b}), \boldsymbol{\kappa}(\boldsymbol{k}, \boldsymbol{b}); \boldsymbol{b}) \\ \boldsymbol{b} &= \boldsymbol{b}_n + \Delta\mu\, \boldsymbol{v}_\beta(\boldsymbol{\beta}(\boldsymbol{\varepsilon}^{\mathrm{e}}, \boldsymbol{k}, \boldsymbol{b}); \boldsymbol{b}) \end{aligned} \tag{32}$$

and the algorithmic Kuhn–Tucker complementary conditions

$$\Delta\mu \geqslant 0\,, \quad \Phi(\boldsymbol{\sigma}(\boldsymbol{\varepsilon}^{\mathrm{e}}, \boldsymbol{b}), \boldsymbol{\kappa}(\boldsymbol{k}, \boldsymbol{b}); \boldsymbol{b}) \leqslant 0, \quad \Delta\mu\, \Phi(\boldsymbol{\sigma}(\boldsymbol{\varepsilon}^{\mathrm{e}}, \boldsymbol{b}), \boldsymbol{\kappa}(\boldsymbol{k}, \boldsymbol{b}); \boldsymbol{b}) = 0 \tag{33}$$

with the elastic trial strain $\boldsymbol{\varepsilon}^{\mathrm{e,tr}} \stackrel{\mathrm{def}}{=} \boldsymbol{\varepsilon} - \boldsymbol{\varepsilon}^{\mathrm{p}}_n$. Elastic unloading (U) is defined by $\Delta\mu = 0$ and $\Phi(\boldsymbol{\sigma}(\boldsymbol{\varepsilon}^{\mathrm{e,tr}}, \boldsymbol{b}_n), \boldsymbol{\kappa}(\boldsymbol{k}_n, \boldsymbol{b}_n); \boldsymbol{b}_n) < 0$, which is the appropriate condition to be checked. Hence, plastic loading (L) is defined by $\Delta\mu > 0$ and $\Phi(\boldsymbol{\sigma}(\boldsymbol{\varepsilon}^{\mathrm{e,tr}}, \boldsymbol{b}_n), \boldsymbol{\kappa}(\boldsymbol{k}_n, \boldsymbol{b}_n); \boldsymbol{b}_n) > 0$. In the latter case, we may replace (32,33) by the residuum equations

$$\begin{aligned} \boldsymbol{R}^{\natural}_{\varepsilon^{\mathrm{e}}}(\boldsymbol{\varepsilon}^{\mathrm{e}}, \boldsymbol{k}, \boldsymbol{b}, \Delta\mu) &= \boldsymbol{\varepsilon}^{\mathrm{e}} - \boldsymbol{\varepsilon}^{\mathrm{e,tr}} + \Delta\mu\, \boldsymbol{v}_\sigma(\boldsymbol{\sigma}(\boldsymbol{\varepsilon}^{\mathrm{e}}, \boldsymbol{b}), \boldsymbol{\kappa}(\boldsymbol{k}, \boldsymbol{b}); \boldsymbol{b}) = \boldsymbol{0} \\ \boldsymbol{R}^{\natural}_{k}(\boldsymbol{\varepsilon}^{\mathrm{e}}, \boldsymbol{k}, \boldsymbol{b}, \Delta\mu) &= \boldsymbol{k} - \boldsymbol{k}_n - \Delta\mu\, \boldsymbol{v}_\kappa(\boldsymbol{\sigma}(\boldsymbol{\varepsilon}^{\mathrm{e}}, \boldsymbol{b}), \boldsymbol{\kappa}(\boldsymbol{k}, \boldsymbol{b}); \boldsymbol{b}) = \boldsymbol{0} \\ \boldsymbol{R}^{\natural}_{b}(\boldsymbol{\varepsilon}^{\mathrm{e}}, \boldsymbol{k}, \boldsymbol{b}, \Delta\mu) &= \boldsymbol{b} - \boldsymbol{b}_n - \Delta\mu\, \boldsymbol{v}_\beta(\boldsymbol{\beta}(\boldsymbol{\varepsilon}^{\mathrm{e}}, \boldsymbol{k}, \boldsymbol{b}); \boldsymbol{b}) = \boldsymbol{0} \\ R^{\natural}_{\mu}(\boldsymbol{\varepsilon}^{\mathrm{e}}, \boldsymbol{k}, \boldsymbol{b}) &= \Phi(\boldsymbol{\sigma}(\boldsymbol{\varepsilon}^{\mathrm{e}}, \boldsymbol{b}), \boldsymbol{\kappa}(\boldsymbol{k}, \boldsymbol{b}); \boldsymbol{b}) = 0 \end{aligned} \tag{34}$$

that we condense in compact notation as

$$\mathbf{R}^{\natural}(\mathbf{X}) = \mathbf{0} \quad \text{with} \quad \mathbf{X} = [\boldsymbol{\varepsilon}^{\mathrm{e}} \;\; \boldsymbol{k} \;\; \boldsymbol{b} \;\; \Delta\mu]^{\mathrm{T}}, \quad \mathbf{R}^{\natural} = [\boldsymbol{R}^{\natural}_{\varepsilon^{\mathrm{e}}} \;\; \boldsymbol{R}^{\natural}_{k} \;\; \boldsymbol{R}^{\natural}_{b} \;\; R^{\natural}_{\mu}]^{\mathrm{T}} \tag{35}$$

For given value $\boldsymbol{\varepsilon}^{\mathrm{e,tr}}$ it is convenient to solve for $\mathbf{X}$ from (35) using Newton iterations; $\mathbf{R}^{\natural} = -\mathbf{J}^{\natural} \circ \mathrm{d}\mathbf{X}$ whereby $\circ$ denotes the proper inner product, with subsequent update of the unknowns, $\mathbf{X} \leftarrow [\mathbf{X} + \mathrm{d}\mathbf{X}]$. In order to increase the degree of symmetry of the Jacobians, we introduce the scaled residuum

$$\boldsymbol{R}_{\varepsilon^{\mathrm{e}}} = \mathbf{E}^{\mathrm{e}} : \boldsymbol{R}^{\natural}_{\varepsilon^{\mathrm{e}}}, \quad \boldsymbol{R}_{k} = \mathbf{H} : \boldsymbol{R}^{\natural}_{k}, \quad \boldsymbol{R}_{b} = \mathbf{G} : \boldsymbol{R}^{\natural}_{b}, \quad R_{\mu} = R_{\mu} \tag{36}$$

(see Appendix A for notational details) which are associated with the scaled Jacobian matrix $\mathbf{J}$ defined as

$$\mathbf{J} = \begin{bmatrix} \mathbf{J}_{\varepsilon^{\mathrm{e}}\varepsilon^{\mathrm{e}}} & \mathbf{J}_{\varepsilon^{\mathrm{e}}k} & \mathbf{J}_{\varepsilon^{\mathrm{e}}b} & \boldsymbol{J}_{\varepsilon^{\mathrm{e}}\mu} \\ \mathbf{J}_{k\varepsilon^{\mathrm{e}}} & \mathbf{J}_{kk} & \mathbf{J}_{kb} & \boldsymbol{J}_{k\mu} \\ \mathbf{J}_{b\varepsilon^{\mathrm{e}}} & \mathbf{J}_{bk} & \mathbf{J}_{bb} & \boldsymbol{J}_{b\mu} \\ \boldsymbol{J}_{\mu\varepsilon^{\mathrm{e}}} & \boldsymbol{J}_{\mu k} & \boldsymbol{J}_{\mu b} & 0 \end{bmatrix} \tag{37}$$

where the specific entries $\mathbf{J}_{[\bullet][\circ]}$ and $\boldsymbol{J}_{[\bullet][\circ]}$ of fourth and second tensorial order are highlighted in Appendix B.

3.1. *Algorithmic tangent stiffness (ATS) tensor*

The ATS-tensor $\mathbf{E}_{\mathrm{a}}^{\mathrm{ep}}$ is defined by the linearized relation

$$\mathrm{d}\boldsymbol{\sigma} = \mathbf{E}_{\mathrm{a}}^{\mathrm{ep}}(\boldsymbol{\varepsilon}) : \mathrm{d}\boldsymbol{\varepsilon} \tag{38}$$

For any given interval $[t_n, t_{n+1}]$ the tangent operator can be computed as follows: We first differentiate $\boldsymbol{\sigma} = \boldsymbol{\sigma}(\boldsymbol{\varepsilon}^{\mathrm{e}}, \boldsymbol{b})$ to obtain

$$\mathrm{d}\boldsymbol{\sigma} = \mathbf{E}^{\mathrm{e}} : \mathrm{d}\boldsymbol{\varepsilon}^{\mathrm{e}} - \mathbf{D}^{\mathrm{e}} : \mathrm{d}\boldsymbol{b} \tag{39}$$

In order to express $\mathrm{d}\boldsymbol{\varepsilon}^{\mathrm{e}}$ and $\mathrm{d}\boldsymbol{b}$ in terms of $\mathrm{d}\boldsymbol{\varepsilon}$, we differentiate the relation $\mathbf{R}^{\natural}(\mathbf{X}, \boldsymbol{\varepsilon}) = \mathbf{0}$ to obtain

$$\mathrm{d}\mathbf{R}^{\natural} = \mathbf{J}^{\natural} \circ \mathrm{d}\mathbf{X} + \mathrm{d}\mathbf{R}^{\natural}|_{\mathrm{X}} = \mathbf{0} \;\Rightarrow\; \mathbf{J}^{\natural} \circ \mathrm{d}\mathbf{X} = -\mathrm{d}\mathbf{R}^{\natural}|_{\mathrm{X}} \tag{40}$$

whereby $\circ$ denotes a proper contraction operator with respect to the format of (37) and the components of $\mathrm{d}\mathbf{R}|_{\mathrm{X}}$ are obtained as

$$\mathrm{d}\boldsymbol{R}^{\natural}_{\varepsilon^{\mathrm{e}}}|_{\mathrm{X}} = -\mathrm{d}\boldsymbol{\varepsilon}, \quad \mathrm{d}\boldsymbol{R}^{\natural}_{k}|_{\mathrm{X}} = \mathbf{0}, \quad \mathrm{d}\boldsymbol{R}^{\natural}_{b}|_{\mathrm{X}} = \mathbf{0}, \quad \mathrm{d}R^{\natural}_{\mu}|_{\mathrm{X}} = \mathbf{0} \tag{41}$$

Upon introducing the scaled differentials, like in (37), we may rephrase $(40)_2$ as

$$\mathbf{J} \circ \mathrm{d}\mathbf{X} = -\mathrm{d}\mathbf{R}|_{\mathrm{X}} \tag{42}$$

from which we obtain (compare Appendix B)

$$\mathrm{d}\boldsymbol{\varepsilon}^{\mathrm{e}} = \mathbf{J}^{\dagger}_{\varepsilon^{\mathrm{e}}\varepsilon^{\mathrm{e}}} : \mathbf{E}^{\mathrm{e}} : \mathrm{d}\boldsymbol{\varepsilon}, \quad \mathrm{d}\boldsymbol{b} = \mathbf{J}^{\dagger}_{b\varepsilon^{\mathrm{e}}} : \mathbf{E}^{\mathrm{e}} : \mathrm{d}\boldsymbol{\varepsilon} \tag{43}$$

where $\mathbf{J}^{\dagger}_{\varepsilon^{\mathrm{e}}\varepsilon^{\mathrm{e}}}$ and $\mathbf{J}^{\dagger}_{b\varepsilon^{\mathrm{e}}}$ are the appropriate parts of the inverse $\mathbf{J}^{\dagger} \overset{\mathrm{def}}{=} \mathbf{J}^{-1}$. Hence, we may combine (43) with (39) to compute

$$\mathbf{E}_{\mathrm{a}}^{\mathrm{ep}} = [\mathbf{E}^{\mathrm{e}} : \mathbf{J}^{\dagger}_{\varepsilon^{\mathrm{e}}\varepsilon^{\mathrm{e}}} - \mathbf{D}^{\mathrm{e}} : \mathbf{J}^{\dagger}_{b\varepsilon^{\mathrm{e}}}] : \mathbf{E}^{\mathrm{e}} \tag{44}$$

In general, it is difficult and time-consuming to derive the ATS-tensor $\mathbf{E}_{\mathrm{a}}^{\mathrm{ep}}$ in closed-form by evaluating the expression in (44). Therefore, it might be preferable to use numerical differentiation to calculate the ATS-tensor (or at least parts of it), e.g. References [24–26].

4. PROTOTYPE MODEL: ISOTROPIC LINEAR ELASTICITY AND VON MISES YIELD CRITERION FOR THE EFFECTIVE MATERIAL

4.1. *Constitutive relations*

We shall consider the situation where the elasticity properties of the undamaged material are isotropic and linear, which is defined by the choice

$$\bar{\Psi}^{\mathrm{e}}(i_1^{(\bar{\varepsilon}^{\mathrm{e}})}, i_2^{(\bar{\varepsilon}^{\mathrm{e}})}) = \tfrac{1}{2} L [i_1^{(\bar{\varepsilon}^{\mathrm{e}})}]^2 + G i_2^{(\bar{\varepsilon}^{\mathrm{e}})} \tag{45}$$

where L and G are the usual Lame's elastic constants. From $(2)_1$ we then obtain the appropriate expression for $\boldsymbol{\sigma}$ as follows – cf. Appendix A for notational details and Appendix B for

the second derivatives of $\bar{\Psi}^{\mathrm{e}}$ –

$$\boldsymbol{\sigma} = [L\boldsymbol{b} \otimes \boldsymbol{b} + 2G\mathbf{P}^{\mathrm{sym}}_{bb}] : \boldsymbol{\varepsilon}^{\mathrm{e}} \tag{46}$$

Next, we consider the simplest format of linear hardening defined by

$$\bar{\Psi}^{\mathrm{p}}(\bar{k}) = \tfrac{1}{2} H \bar{k}^2 \tag{47}$$

where H is the constant hardening modulus of the undamaged material for the uniaxial stress state. From $(3)_1$ we then obtain

$$\boldsymbol{\kappa} = -H[\boldsymbol{b} \otimes \boldsymbol{b}] : \boldsymbol{k} \tag{48}$$

Since the tensor $\boldsymbol{b}$ is incorporated in (48), it appears that the simple choice in (47) allows for anisotropic effects in the nominal hardening.

Remark 4.1
In terms of effective quantities, we may combine the definition of $\bar{\kappa}$ in (27) with (23) to conclude that (48) is equivalent to $\bar{\kappa} = -H\bar{k}$, which is the usual expression of the scalar drag-stress for the undamaged material.

Furthermore, from $(3)_2$ we now obtain for the integrity stress

$$\boldsymbol{\beta} = -[L\boldsymbol{\varepsilon}^{\mathrm{e}} \otimes \boldsymbol{\varepsilon}^{\mathrm{e}} + 2G\mathbf{P}^{\mathrm{sym}}_{\varepsilon^{\mathrm{e}}\varepsilon^{\mathrm{e}}} + H\boldsymbol{k} \otimes \boldsymbol{k}] : \boldsymbol{b} \tag{49}$$

In the sequel we shall adopt the von Mises yield function with linear hardening, which is defined by

$$\bar{\Phi}(i_1^{(\bar{\sigma})}, i_2^{(\bar{\sigma})}, \bar{\kappa}) = \bar{\sigma}_{\mathrm{e}}(i_1^{(\bar{\sigma})}, i_2^{(\bar{\sigma})}) - \sigma_{\mathrm{Y}} - \bar{\kappa} \tag{50}$$

where $\bar{\sigma}_{\mathrm{e}}$ denotes the equivalent stress (compare Appendix A for notational details)

$$\bar{\sigma}_{\mathrm{e}} = \sqrt{\frac{3}{2} j_2^{(\bar{\sigma})}}, \quad j_2^{(\bar{\sigma})} \overset{\mathrm{def}}{=} i_2^{(\bar{\sigma})} - \frac{1}{3}[i_1^{(\bar{\sigma})}]^2 = \boldsymbol{\sigma} : \mathbf{P}^{\mathrm{sym}}_{b^{-1}b^{-1},\mathrm{dev}} : \boldsymbol{\sigma} \tag{51}$$

Hence, we may express the gradients $\boldsymbol{v}_\sigma$ and $\boldsymbol{v}_\kappa$ as

$$\boldsymbol{v}_\sigma = \frac{3}{2\bar{\sigma}_{\mathrm{e}}} \mathbf{P}^{\mathrm{sym}}_{b^{-1}b^{-1},\mathrm{dev}} : \boldsymbol{\sigma} \quad \text{and} \quad \boldsymbol{v}_\kappa = -\frac{1}{3}\boldsymbol{b}^{-1} \tag{52}$$

For the evolution law for damage which defines the disintegration, a possible and most obvious choice is the quadratic format

$$\bar{\Gamma}(i_1^{(\bar{\beta})}, i_2^{(\bar{\beta})}) = \tfrac{1}{2}\eta_1 [i_1^{(\bar{\beta})}]^2 + \tfrac{1}{2}\eta_2 i_2^{(\bar{\beta})} \tag{53}$$

where η_1, η_2 are constant parameters. This gives $\boldsymbol{v}_\beta$ finally as

$$\boldsymbol{v}_\beta = [\eta_1 \boldsymbol{b} \otimes \boldsymbol{b} + \eta_2 \mathbf{P}^{\mathrm{sym}}_{bb}] : \boldsymbol{\beta} \tag{54}$$

Even though this model conforms to the advocated framework, it turns out that the predictive capability of (54) is too restrictive to serve as a good model in practice (for many materials).

We shall therefore adopt the generalization of (54) as follows:

$$\boldsymbol{v}_\beta = \mathbf{R}^{(m)}(\boldsymbol{b}) : \boldsymbol{\beta} \quad \text{with} \quad \mathbf{R}^{(m)} = \eta_1 \boldsymbol{b}^m \otimes \boldsymbol{b}^m + \eta_2 \mathbf{P}^{\text{sym}}_{\boldsymbol{b}^m \boldsymbol{b}^m} \tag{55}$$

where the exponent m is an additional constitutive parameter. It is noted that $\mathbf{R}^{(m)}$ is positive definite as long as $\boldsymbol{b}$ is positive, which ensures that positive dissipation is generated from the damage process. Clearly, (54) is retrieved for $m = 1$. The widely used damage model by Lemaitre [1], which is usually employed in conjunction with the postulate of strain equivalence, is closely resembled if we set $m = -1$. Nevertheless, the choice $m \neq 1$ is not consistent with the strain energy equivalence based on the concept of an effective configuration, i.e. the 'damage rule' derived from (55) is not derivable from a scalar invariant function of the format $\bar{\Gamma} = \bar{\Gamma}(i_1^{(\bar{\beta})}, i_2^{(\bar{\beta})}, i_3^{(\bar{\beta})})$. Rather, the choice $m \neq 1$ is motivated solely from the resulting improvement of the predictive capability. A comparison of $m = 1$ and -2 is included in the next section.

For the numerical implementation of the proposed prototype model, it is possible to give the Jacobian $\mathbf{J}$ in closed-form, cf. Appendix C. (This is done in the present implementation with the exception of one single matrix element of $\mathbf{J}$, cf. Appendix C.)

Remark 4.2
Although the effective quantities are introduced via the mapping $\bar{\boldsymbol{F}}$, in practice there is no need to compute $\bar{\boldsymbol{F}}$ or any of the effective quantities in the present case of an isotropic effective configuration. All the relevant relations are expressed in terms of variables pertinent to the nominal configuration $\mathscr{B}$. However, if the effective configuration is anisotropic ($\bar{\boldsymbol{b}} \neq \bar{\boldsymbol{I}}$), then the rotation involved in $\bar{\boldsymbol{F}}$ will enter the formulation explicitly.

5. COMPUTATIONAL RESULTS

5.1. Preliminaries

In the numerical investigations of the prototype model described in Section 4 the following academic values of material parameters are used:

$$\sigma_Y = 1, \quad \frac{E}{\sigma_Y} = 400, \quad \frac{H}{\sigma_Y} = 100, \quad \nu = 0.3, \quad \frac{\eta_1}{\sigma_Y} = \frac{\eta_2}{\sigma_Y} = 2 \cdot 10^3 \tag{56}$$

5.2. Stress–strain curves

In Figures 1 and 2 we compare the model performance in uniaxial stress with $\sigma_{ij} = 0 \ \forall ij \neq 11$ for different values of the exponent m. The strain ε_{11} is controlled and the other strains ε_{ij} with $ij \neq 11$ are obtained from the uniaxial stress condition. In the figures both the development of stress σ_{11} and damage $\dot{\boldsymbol{b}}$ are shown. As alluded to above, a more ductile behaviour is shown for $m = 1$ as compared to $m = -2$. However, the limit $\sigma_{11} = 0$ is only reached asymptotically; indeed, by analysing the one-dimensional case, this can be shown to be a consequence of the postulate of energy equivalence for the particular choice of damage law in (55). Figures 3 and 4 show the response when both ε_{11} and ε_{22} are controlled, with $\varepsilon_{11} = \varepsilon_{22}$, under the condition of plane stress, $\sigma_{i3} = \sigma_{3j} = 0 \ \forall i, j$. Again, similar conclusions as from Figures 1 and 2 can be drawn. The anisotropic nature of the damage is clearly seen from the different principal values of $\boldsymbol{b}$.

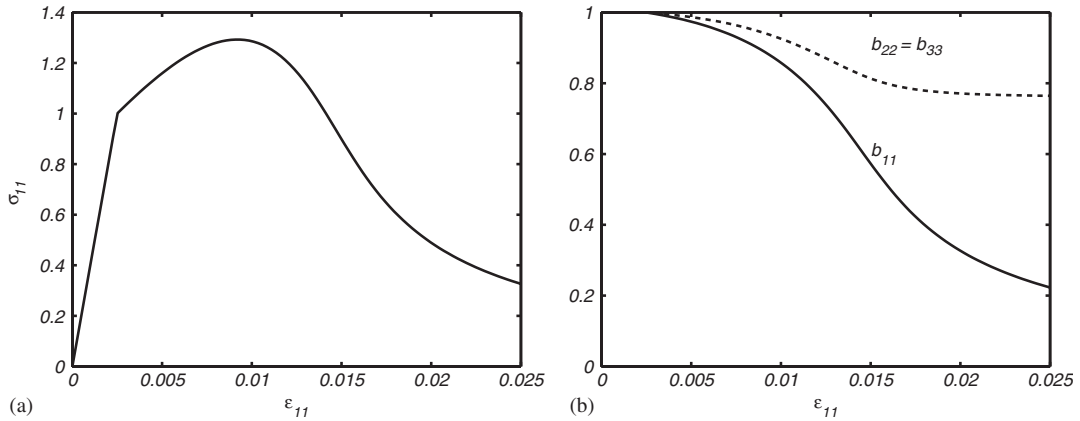

Figure 1. Strain-driven loading at uniaxial stress with $m = -2$: (a) stress–strain behaviour; and (b) damage development.

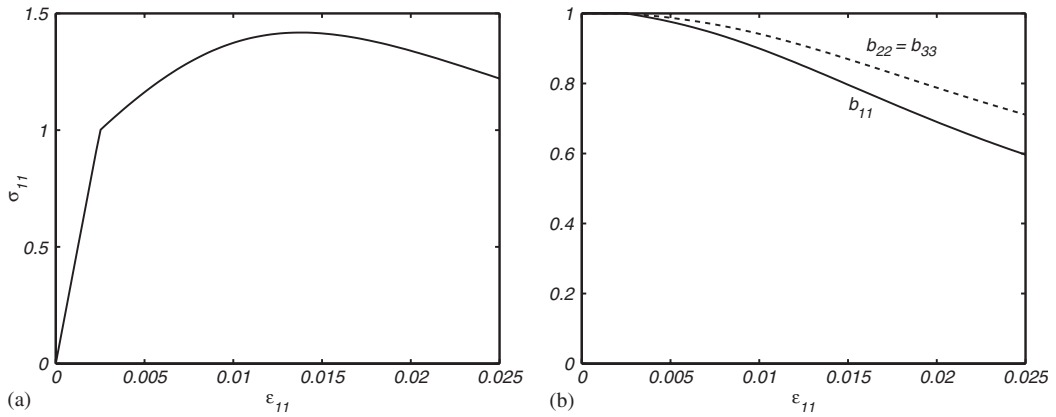

Figure 2. Strain-driven loading at uniaxial stress with $m = 1$: (a) stress–strain behaviour; and (b) damage development.

5.3. *Flow-surfaces*

In Figures 5–10 it is shown how the yield surface changes with deformation. In each figure the yield surface is plotted for 3 occasions during the deformation with respect to Cartesian co-ordinates σ_{ij} with $\sigma_{ij} = 0$ for $i \neq j$. The deformation is strain-controlled with different angles $\phi = \tan^{-1}(\varepsilon_{22}/\varepsilon_{11})$ under the condition of plane stress. Again the anisotropy and its development is clearly visible from the rotation and elongation of the initially isotropic v. Mises ellipse.

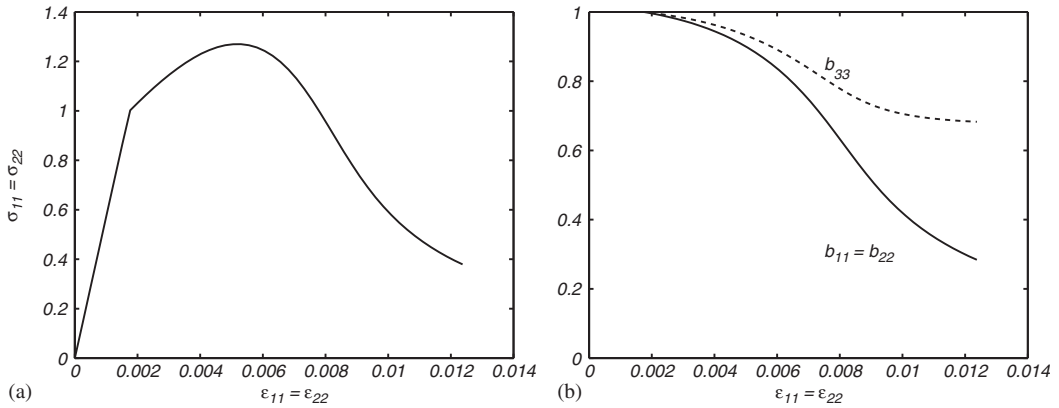

Figure 3. Strain-driven loading at plane stress with $m = -2$: (a) stress–strain behaviour; and (b) damage development.

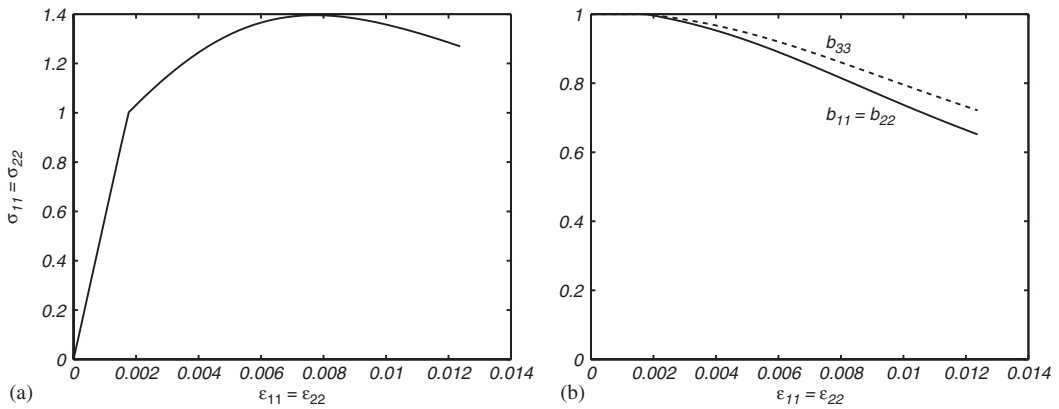

Figure 4. Strain-driven loading at plane stress with $m = 1$: (a) stress–strain behaviour; and (b) damage development.

5.4. Sequence of shear and normal loading of a simple structure—FE results

In order to investigate how the proposed model performs in a structural problem, in particular with respect to the induced anisotropy that is brought about by accumulation of damage, we shall consider the square panel in Figure 11. A fixed finite element subdivision of standard linear approximation triangles was used. The material data are $m = -2$ in addition to those in (56).

The loading was of two types and applied in two sequential steps: In the first step the upper surface of the panel was subjected to a uniform horizontal displacement, while the vertical displacements are left free. The resulting horizontal force versus horizontal displacement is shown in Figure 11(b) for loading and unloading, whereas the deformed meshes at the points

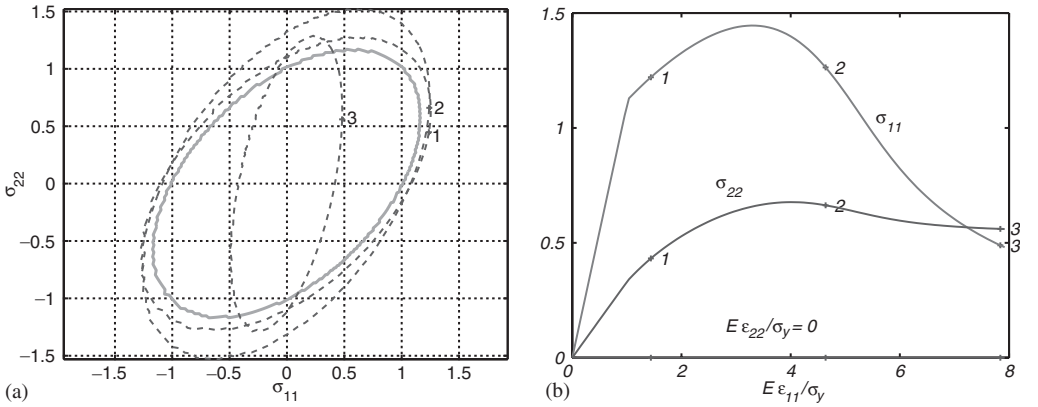

Figure 5. Strain-driven loading with $\varepsilon_{22} = 0$ and plane stress, $m = -2$: (a) development of the yield surface (initial yield surface); and (b) stress–strain behaviour.

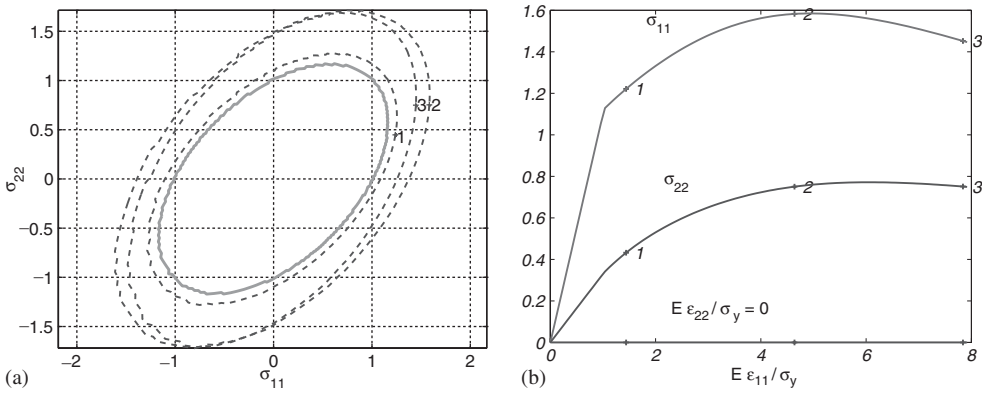

Figure 6. Strain-driven loading with $\varepsilon_{22} = 0$ and plane stress, $m = 1$: (a) development of the yield surface (initial yield surface); and (b) stress–strain behaviour.

of unloading and fully removed load are shown in Figure 12 (whereby the displacements are magnified 25 times). Hence, Figure 12(b) shows the residual configuration, whereas Figure 13 shows the residual stress and damage states in terms of the principal values of $\boldsymbol{\sigma}$ and $\boldsymbol{I} - \boldsymbol{b}$. Two conclusions can be drawn from Figure 13(a) and 13(b): the principal directions of the stress $\boldsymbol{\sigma}$ and $\boldsymbol{I} - \boldsymbol{b}$ do not coincide; and a localization band can be detected from the damage distribution.

In the second step of the loading process, the upper surface was subjected to an additional uniform vertical displacement, while the horizontal displacements are free. The resulting vertical force versus vertical displacement for the left upper corner is shown in Figure 14(a) for loading up to a certain amount of displacement. It appears from the deformation pattern in Figure 14(b) that strong localization in a nearly horizontal band was encountered during

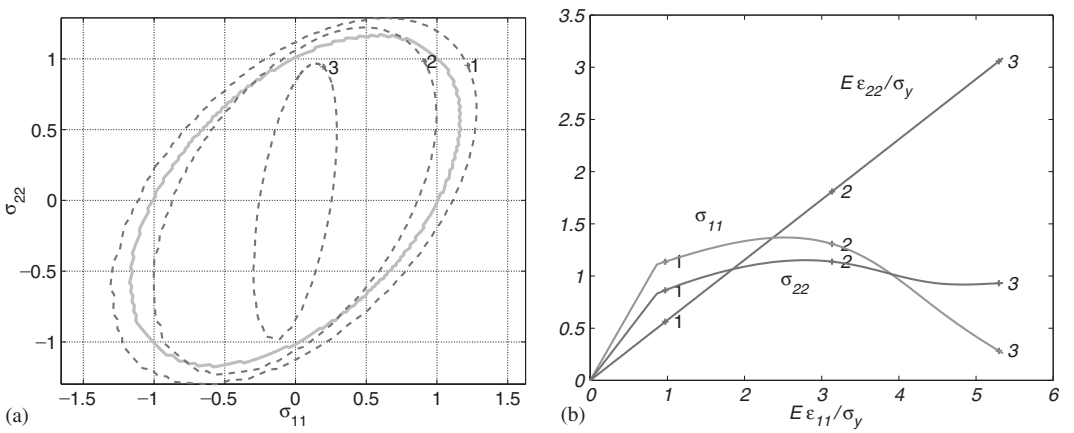

Figure 7. Strain-driven loading with $\varepsilon_{22}/\varepsilon_{11} = \tan(30^\circ)$ and plane stress, $m = -2$: (a) development of the yield surface (initial yield surface); and (b) stress–strain behaviour.

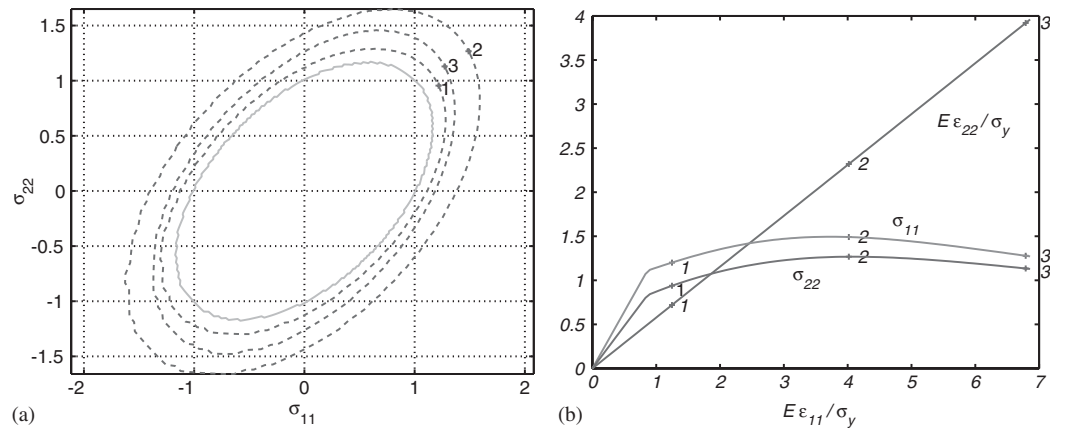

Figure 8. Strain-driven loading with $\varepsilon_{22}/\varepsilon_{11} = \tan(30^\circ)$ and plane stress, $m = 1$: (a) development of the yield surface (initial yield surface); and (b) stress–strain behaviour.

this loading step. Moreover, the localization is reflected also by the damage distribution see Figure 15(b), since damage grows only in the band-shaped zone. It is also seen that the principal values of $\boldsymbol{b}$ become more aligned with the vertical (loading) and horizontal directions, although this feature is less pronounced. At this point we remark that no specific provision is made for localization capturing. Hence, it can be expected that the load–displacement response relation in the post-peak region of Figure 14(a) is strongly mesh-dependent. This issue falls, however, outside the scope of the present paper and constitutes a topic of our future research.

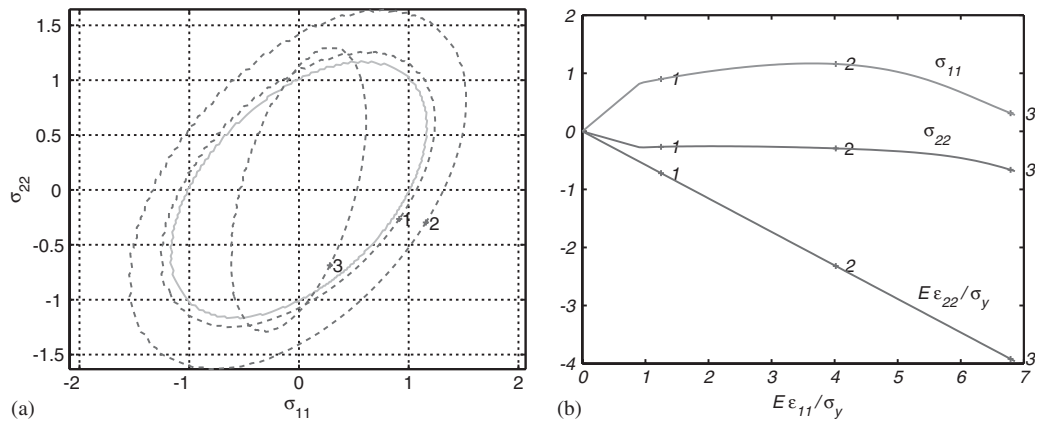

Figure 9. Strain-driven loading with $\varepsilon_{22}/\varepsilon_{11} = \tan(-30^\circ)$ and plane stress, $m = -2$: (a) development of the yield surface (initial yield surface); and (b) stress–strain behaviour.

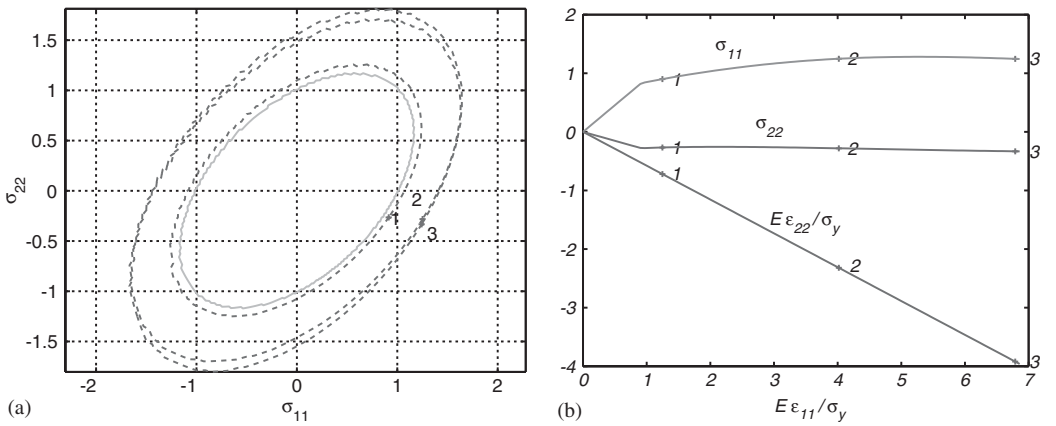

Figure 10. Strain-driven loading with $\varepsilon_{22}/\varepsilon_{11} = \tan(-30^\circ)$ and plane stress, $m = 1$: (a) development of the yield surface (initial yield surface); and (b) stress–strain behaviour.

6. CONCLUDING REMARKS AND FUTURE WORK

The described model framework for anisotropic damage kinetically coupled to inelastic deformations was presented while restricting the formulation to initial isotropy and isotropic hardening of the virgin material in the absence of degradation. The presented numerical results demonstrate that it is possible to represent the deformation-induced anisotropy such that the rate of damage evolution is larger in the direction of large stresses. However, it remains to carry out tests and calibrate a specific model for a given material and given loading conditions in order to assess the predictive capability for practical usage. Future improvements should include kinematic hardening, the effect of microcrack closure and reopening (MCR), and the

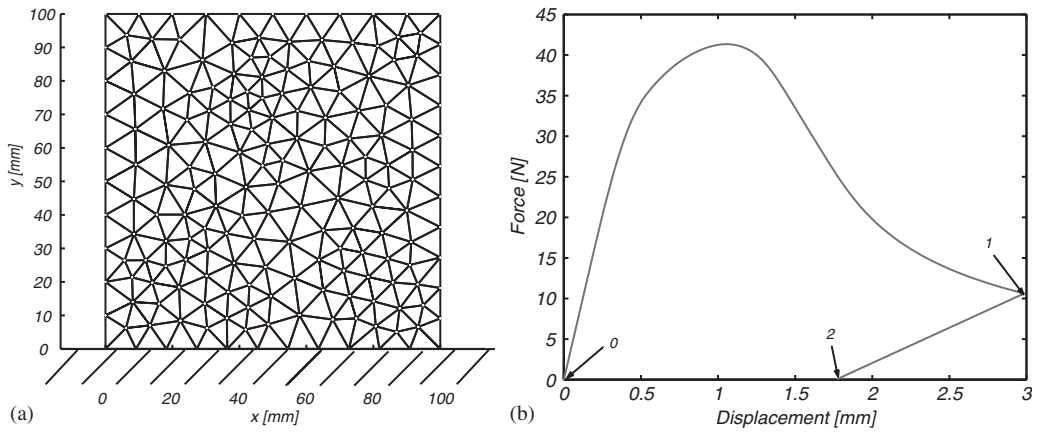

Figure 11. The first step of the loading: The displacement of the upper nodes is increased $0 \rightarrow 1$, followed by complete unloading $1 \rightarrow 2$.

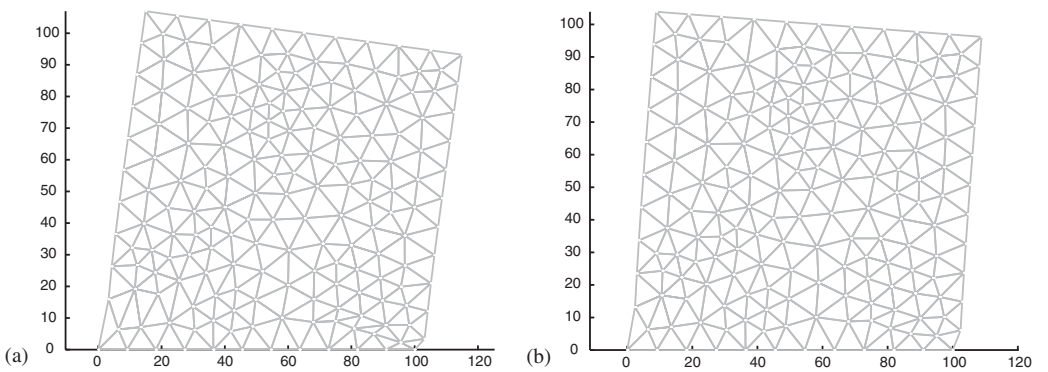

Figure 12. Deformed mesh at: (a) state 1; and (b) state 2.

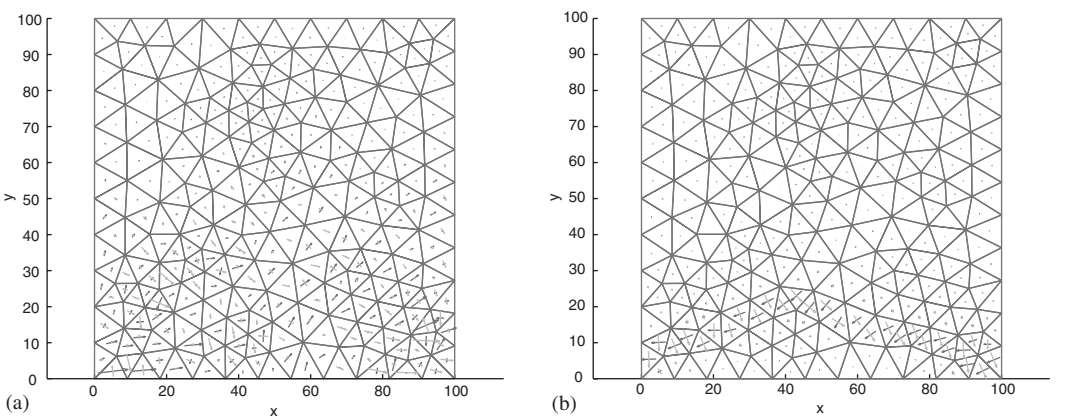

Figure 13. Map at state 2: (a) of the principal stresses; and (b) principal values (in the plane) of $\boldsymbol{I} - \boldsymbol{b}$.

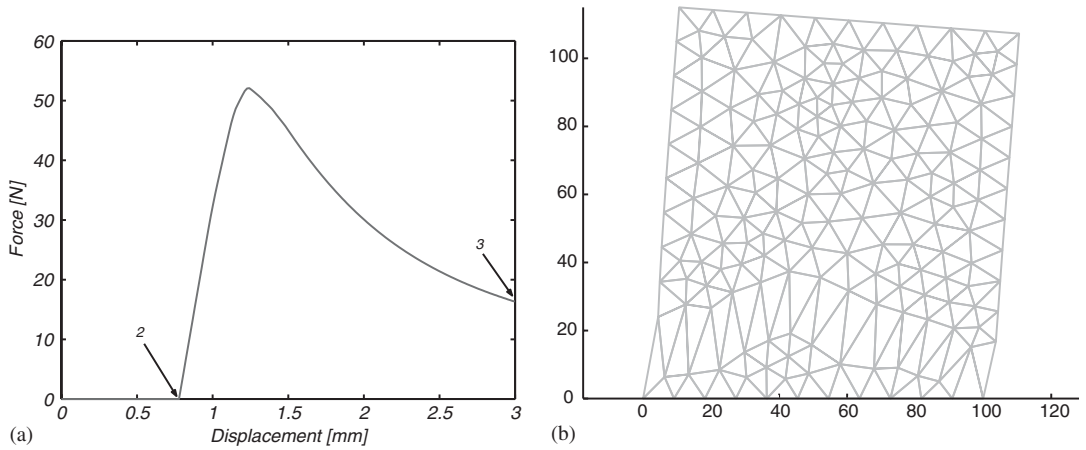

Figure 14. The second step of the loading: The displacement of the upper nodes is increased $2 \rightarrow 3$.

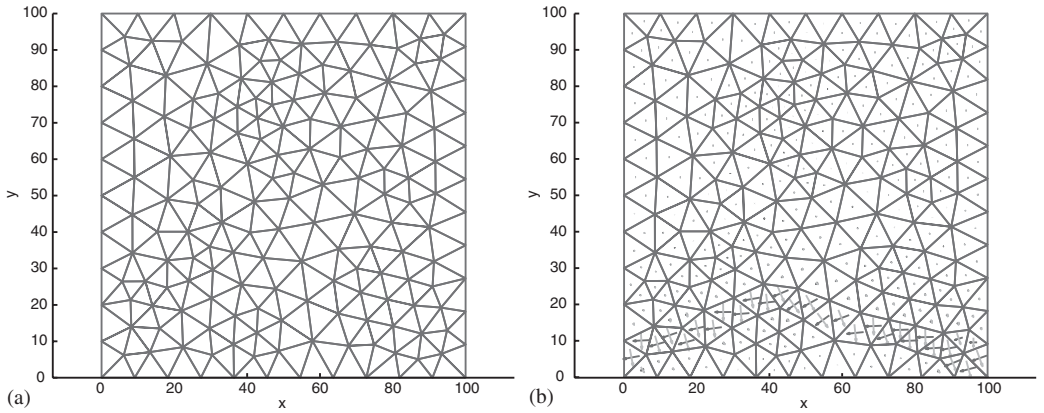

Figure 15. Map at state 3: (a) of the principal stresses; and (b) principal values (in the plane) of $\boldsymbol{I} - \boldsymbol{b}$.

extension to truly large strains so that the model framework can be used in, for example, material forming situations. However, neither of these tasks is trivial.

APPENDIX A: NOTATION

For any two second-order symmetric tensors $\boldsymbol{A}$ and $\boldsymbol{B}$, the symmetric fourth order tensor $\mathbf{P}_{AB}^{\mathrm{sym}}$ is defined as

$$\begin{aligned} \mathbf{P}_{AB}^{\mathrm{sym}} &= \tfrac{1}{4}[\boldsymbol{A} \overline{\otimes} \boldsymbol{B} + \boldsymbol{A} \underline{\otimes} \boldsymbol{B} + \boldsymbol{B} \overline{\otimes} \boldsymbol{A} + \boldsymbol{B} \underline{\otimes} \boldsymbol{A}] \\ \mathbf{P}_{AA}^{\mathrm{sym}} &= \tfrac{1}{2}[\boldsymbol{A} \overline{\otimes} \boldsymbol{A} + \boldsymbol{A} \underline{\otimes} \boldsymbol{A}] \end{aligned} \tag{A1}$$

whereby the non-standard dyadic products $\overline{\otimes}$ and $\underline{\otimes}$ read

$$[\boldsymbol{A}\,\overline{\otimes}\,\boldsymbol{B}]_{ijkl}=[\boldsymbol{A}]_{ik}[\boldsymbol{B}]_{jl},\quad [\boldsymbol{A}\,\underline{\otimes}\,\boldsymbol{B}]_{ijkl}=[\boldsymbol{A}]_{il}[\boldsymbol{B}]_{jk} \tag{A2}$$

Thus, the usual fourth-order identity tensor $\mathbf{I}^{\mathrm{sym}}$ is obtained as $\mathbf{I}^{\mathrm{sym}}=\mathbf{P}_{II}^{\mathrm{sym}}$. We also introduce a deviatoric fourth-order tensor as

$$\mathbf{P}_{AA,\mathrm{dev}}^{\mathrm{sym}}=\mathbf{P}_{AA}^{\mathrm{sym}}-\frac{1}{n_{\mathrm{dim}}}\,\boldsymbol{A}\otimes\boldsymbol{A} \tag{A3}$$

whereby n_{dim} denotes the appropriate space-dimension. Finally, we introduce the abbreviated notations

$$\boldsymbol{\Psi}_{[\bullet][\circ]}=\frac{\partial^2\Psi}{\partial[\bullet]\,\partial[\circ]},\quad \boldsymbol{\Phi}^{*}_{[\bullet][\circ]}=\frac{\partial^2\Phi^{*}}{\partial[\bullet]\,\partial[\circ]}$$

and

$$\begin{aligned}
\mathbf{E}^{\mathrm{e}} &\overset{\mathrm{def}}{=} \boldsymbol{\Psi}_{\varepsilon^{\mathrm{e}}\varepsilon^{\mathrm{e}}}=\frac{\partial\boldsymbol{\sigma}}{\partial\boldsymbol{\varepsilon}^{\mathrm{e}}}\\
-\mathbf{D}^{\mathrm{e}} &\overset{\mathrm{def}}{=} \boldsymbol{\Psi}_{\varepsilon^{\mathrm{e}}b}=\frac{\partial\boldsymbol{\sigma}}{\partial\boldsymbol{b}}\\
\mathbf{H} &\overset{\mathrm{def}}{=} \boldsymbol{\Psi}_{kk}=-\frac{\partial\boldsymbol{\kappa}}{\partial\boldsymbol{k}}\\
-\mathbf{Y} &\overset{\mathrm{def}}{=} \boldsymbol{\Psi}_{kb}=-\frac{\partial\boldsymbol{\kappa}}{\partial\boldsymbol{b}}=-\left[\frac{\partial\boldsymbol{\beta}}{\partial\boldsymbol{k}}\right]^{\mathrm{T}}\\
\mathbf{G} &\overset{\mathrm{def}}{=} \boldsymbol{\Psi}_{bb}=-\frac{\partial\boldsymbol{\beta}}{\partial\boldsymbol{b}}
\end{aligned} \tag{A4}$$

APPENDIX B: USEFUL DERIVATIVES

In the sequel we summarize some useful derivatives referring to the general framework in Sections 2 and 3:

Derivatives of the first and second strain invariants:

$$\begin{aligned}
&\frac{\partial i_1^{(\bar{\varepsilon}^{\mathrm{e}})}}{\partial\boldsymbol{\varepsilon}^{\mathrm{e}}}=\boldsymbol{b},\quad \frac{\partial i_2^{(\bar{\varepsilon}^{\mathrm{e}})}}{\partial\boldsymbol{\varepsilon}^{\mathrm{e}}}=2\boldsymbol{b}\cdot\boldsymbol{\varepsilon}^{\mathrm{e}}\cdot\boldsymbol{b}=2\mathbf{P}_{bb}^{\mathrm{sym}}:\boldsymbol{\varepsilon}^{\mathrm{e}}\\
&\frac{\partial i_1^{(\bar{\varepsilon}^{\mathrm{e}})}}{\partial\boldsymbol{b}}=\boldsymbol{\varepsilon},\quad \frac{\partial i_2^{(\bar{\varepsilon}^{\mathrm{e}})}}{\partial\boldsymbol{b}}=2\boldsymbol{\varepsilon}^{\mathrm{e}}\cdot\boldsymbol{b}\cdot\boldsymbol{\varepsilon}^{\mathrm{e}}=2\mathbf{P}_{\varepsilon^{\mathrm{e}}\varepsilon^{\mathrm{e}}}^{\mathrm{sym}}:\boldsymbol{b}
\end{aligned} \tag{B1}$$

Derivatives of the first and second stress invariants:

$$\begin{aligned}
&\frac{\partial i_1^{(\bar{\sigma})}}{\partial\boldsymbol{\sigma}}=\boldsymbol{b}^{-1},\quad \frac{\partial i_2^{(\bar{\sigma})}}{\partial\boldsymbol{\sigma}}=2\boldsymbol{b}^{-1}\cdot\boldsymbol{\sigma}\cdot\boldsymbol{b}^{-1}=2\mathbf{P}_{b^{-1}b^{-1}}^{\mathrm{sym}}:\boldsymbol{\sigma}\\
&\frac{\partial i_1^{(\bar{\sigma})}}{\partial\boldsymbol{b}^{-1}}=\boldsymbol{\sigma},\qquad \frac{\partial i_2^{(\bar{\sigma})}}{\partial\boldsymbol{b}^{-1}}=2\boldsymbol{\sigma}\cdot\boldsymbol{b}^{-1}\cdot\boldsymbol{\sigma}=2\,\mathbf{P}_{\sigma\sigma}^{\mathrm{sym}}:\boldsymbol{b}^{-1}
\end{aligned} \tag{B2}$$

Derivatives of the first and second integrity-stress invariants:

$$\frac{\partial i_1^{(\bar{\beta})}}{\partial \boldsymbol{\beta}} = \boldsymbol{b}, \quad \frac{\partial i_2^{(\bar{\beta})}}{\partial \boldsymbol{\beta}} = 2\boldsymbol{b}\cdot\boldsymbol{\beta}\cdot\boldsymbol{b} = 2\mathbf{P}_{bb}^{\mathrm{sym}} : \boldsymbol{\beta}$$
$$\frac{\partial i_1^{(\bar{\beta})}}{\partial \boldsymbol{b}} = \boldsymbol{\beta}, \quad \frac{\partial i_2^{(\bar{\beta})}}{\partial \boldsymbol{b}} = 2\boldsymbol{\beta}\cdot\boldsymbol{b}\cdot\boldsymbol{\beta} = 2\mathbf{P}_{\beta\beta}^{\mathrm{sym}} : \boldsymbol{b} \tag{B3}$$

Derivatives of the first hardening invariant:

$$\frac{\partial \bar{k}}{\partial \boldsymbol{k}} = \boldsymbol{b}, \quad \frac{\partial \bar{k}}{\partial \boldsymbol{b}} = \boldsymbol{k} \tag{B4}$$

Entries of the Jacobian $\mathbf{J}$ *in* (37):

$$\begin{aligned}
\mathbf{J}_{\varepsilon^e\varepsilon^e} &= \boldsymbol{\Psi}_{\varepsilon^e\varepsilon^e} + \Delta\mu\, \boldsymbol{\Psi}_{\varepsilon^e\varepsilon^e} : \boldsymbol{\Phi}^*_{\sigma\sigma} : \boldsymbol{\Psi}_{\varepsilon^e\varepsilon^e} \\
\mathbf{J}_{\varepsilon^e k} &= -\Delta\mu\, \boldsymbol{\Psi}_{\varepsilon^e\varepsilon^e} : \boldsymbol{\Phi}^*_{\sigma\kappa} : \boldsymbol{\Psi}_{kk} = \mathbf{J}^{\mathrm{T}}_{k\varepsilon^e} \\
\mathbf{J}_{\varepsilon^e b} &= \Delta\mu[\boldsymbol{\Psi}_{\varepsilon^e\varepsilon^e} : \boldsymbol{\Phi}^*_{\sigma\sigma} : \boldsymbol{\Psi}_{\varepsilon^e b} - \boldsymbol{\Psi}_{\varepsilon^e\varepsilon^e} : \boldsymbol{\Phi}^*_{\sigma\kappa} : \boldsymbol{\Psi}_{kb} + \boldsymbol{\Psi}_{\varepsilon^e\varepsilon^e} : \boldsymbol{\Phi}^*_{\sigma b}] \neq \mathbf{J}^{\mathrm{T}}_{b\varepsilon^e} \\
\boldsymbol{J}_{\varepsilon^e\mu} &= \boldsymbol{\Psi}_{\varepsilon^e\varepsilon^e} : \boldsymbol{v}_\sigma = \boldsymbol{J}_{\mu\varepsilon^e} \\
\mathbf{J}_{k\varepsilon^e} &= -\Delta\mu \boldsymbol{\Psi}_{kk} : \boldsymbol{\Phi}^*_{\kappa\sigma} : \boldsymbol{\Psi}_{\varepsilon^e\varepsilon^e} = \mathbf{J}^{\mathrm{T}}_{k\varepsilon^e} \\
\mathbf{J}_{kk} &= \boldsymbol{\Psi}_{kk} + \Delta\mu \boldsymbol{\Psi}_{kk} : \boldsymbol{\Phi}^*_{\kappa\kappa} : \boldsymbol{\Psi}_{kk} \\
\mathbf{J}_{kb} &= -\Delta\mu[\boldsymbol{\Psi}_{kk} : \boldsymbol{\Phi}^*_{\kappa\sigma} : \boldsymbol{\Psi}_{\varepsilon^e b} - \boldsymbol{\Psi}_{kk} : \boldsymbol{\Phi}^*_{\kappa\kappa} : \boldsymbol{\Psi}_{kb} + \boldsymbol{\Psi}_{kk} : \boldsymbol{\Phi}^*_{\kappa b}] \neq \mathbf{J}^{\mathrm{T}}_{bk} \\
\boldsymbol{J}_{k\mu} &= -\boldsymbol{\Psi}_{kk} : \boldsymbol{v}_\kappa = \boldsymbol{J}_{\mu k} \\
\mathbf{J}_{b\varepsilon^e} &= \Delta\mu \boldsymbol{\Psi}_{bb} : \boldsymbol{\Phi}^*_{\beta\beta} : \boldsymbol{\Psi}_{b\varepsilon^e} \neq \mathbf{J}^{\mathrm{T}}_{\varepsilon^e b} \\
\mathbf{J}_{bk} &= \Delta\mu \boldsymbol{\Psi}_{bb} : \boldsymbol{\Phi}^*_{\beta\beta} : \boldsymbol{\Psi}_{bk} \neq \mathbf{J}^{\mathrm{T}}_{kb} \\
\mathbf{J}_{bb} &= \boldsymbol{\Psi}_{bb} + \Delta\mu[\boldsymbol{\Psi}_{bb} : \boldsymbol{\Phi}^*_{\beta\beta} : \boldsymbol{\Psi}_{bb} - \boldsymbol{\Psi}_{bb} : \boldsymbol{\Phi}^*_{\beta b}] \\
\boldsymbol{J}_{b\mu} &= -\boldsymbol{\Psi}_{bb} : \boldsymbol{v}_\beta \neq \boldsymbol{J}_{\mu b} \\
\boldsymbol{J}_{\mu\varepsilon^e} &= \boldsymbol{v}_\sigma : \boldsymbol{\Psi}_{\varepsilon^e\varepsilon^e} = \boldsymbol{J}_{\varepsilon^e\mu} \\
\boldsymbol{J}_{\mu k} &= -\boldsymbol{v}_\kappa : \boldsymbol{\Psi}_{kk} = \boldsymbol{J}_{k\mu} \\
\boldsymbol{J}_{\mu b} &= \boldsymbol{v}_\sigma : \boldsymbol{\Psi}_{\varepsilon^e b} - \boldsymbol{v}_\kappa : \boldsymbol{\Psi}_{kb} + \boldsymbol{v}_b \neq \boldsymbol{J}_{b\mu}
\end{aligned} \tag{B5}$$

APPENDIX C: SELECTED CLOSED-FORM EXPRESSIONS OF THE PROTOTYPE MODEL

In the sequel we summarize some useful derivatives which are used in Section 4 in order to compute tangent operators:

Second derivatives of the prototype free energy function in (45, 47):

$$\begin{aligned}
\mathbf{E}^{\mathrm{e}} &= L\boldsymbol{b}\otimes\boldsymbol{b} + 2G\mathbf{P}^{\mathrm{sym}}_{bb}\\
-\mathbf{D}^{\mathrm{e}} &= L[i_1^{(\bar{\varepsilon}^{\mathrm{e}})}\mathbf{I}^{\mathrm{sym}} + \boldsymbol{b}\otimes\boldsymbol{\varepsilon}^{\mathrm{e}}] + 4G\mathbf{P}^{\mathrm{sym}}_{Ic_1}\\
\mathbf{H} &= H\boldsymbol{b}\otimes\boldsymbol{b}\\
-\mathbf{Y} &= H[i_1^{(\bar{k})}\mathbf{I}^{\mathrm{sym}} + \boldsymbol{b}\otimes\boldsymbol{k}]\\
\mathbf{G} &= L\boldsymbol{\varepsilon}^{\mathrm{e}}\otimes\boldsymbol{\varepsilon}^{\mathrm{e}} + 2G\mathbf{P}^{\mathrm{sym}}_{\boldsymbol{\varepsilon}^{\mathrm{e}}\boldsymbol{\varepsilon}^{\mathrm{e}}} + H\boldsymbol{k}\otimes\boldsymbol{k}
\end{aligned} \tag{C1}$$

with $\boldsymbol{c}_1 \overset{\mathrm{def}}{=} \boldsymbol{b}\cdot\boldsymbol{\varepsilon}^{\mathrm{e}}$. It appears that $\mathbf{D}^{\mathrm{e}}$ and $\mathbf{Y}$ do not possess major symmetry due to the terms $\boldsymbol{b}\otimes\boldsymbol{\varepsilon}^{\mathrm{e}}$ and $\boldsymbol{b}\otimes\boldsymbol{k}$, respectively. In addition, it appears that $\mathbf{E}^{\mathrm{e}}$ assumes the usual format for isotropic linear elasticity in the virgin state, i.e. when $\boldsymbol{b}=\boldsymbol{I}$.

Second derivatives of the yield function in (50) *of the prototype model*:

$$\begin{aligned}
\boldsymbol{\Phi}^*_{\sigma\sigma} &= \frac{3}{2\bar{\sigma}_{\mathrm{e}}}(\mathbf{P}^{\mathrm{sym}}_{b^{-1}b^{-1},\mathrm{dev}} - \tfrac{2}{3}\boldsymbol{v}_\sigma\otimes\boldsymbol{v}_\sigma)\\
\boldsymbol{\Phi}^*_{\sigma b} &= \frac{3}{2\bar{\sigma}_{\mathrm{e}}}\left(\frac{\partial}{\partial\boldsymbol{b}^{-1}}(\mathbf{P}^{\mathrm{sym}}_{b^{-1}b^{-1},\mathrm{dev}}:\boldsymbol{\sigma}) : \frac{\partial\boldsymbol{b}^{-1}}{\partial\boldsymbol{b}} - \frac{1}{\bar{\sigma}_{\mathrm{e}}}(\mathbf{P}^{\mathrm{sym}}_{b^{-1}b^{-1},\mathrm{dev}}:\boldsymbol{\sigma})\otimes\frac{\partial\bar{\sigma}_{\mathrm{e}}}{\partial\boldsymbol{b}}\right)\\
\boldsymbol{\Phi}^*_{\kappa\sigma} &= \mathbf{0}\\
\boldsymbol{\Phi}^*_{\kappa\kappa} &= \mathbf{0}\\
\boldsymbol{\Phi}^*_{\kappa b} &= -\frac{1}{3}\frac{\partial\boldsymbol{b}^{-1}}{\partial\boldsymbol{b}}\\
\boldsymbol{\Phi}^*_{\beta\beta} &= \mathbf{R}^{(m)}\\
\boldsymbol{\Phi}^*_{\beta b} &= \boldsymbol{\Phi}^*_{\beta b^m} : \frac{\partial\boldsymbol{b}^m}{\partial\boldsymbol{b}}
\end{aligned} \tag{C2}$$

where

$$\begin{aligned}
\frac{\partial\boldsymbol{b}^{-1}}{\partial\boldsymbol{b}} &= -\mathbf{P}^{\mathrm{sym}}_{b^{-1}b^{-1}}\\
\frac{\partial\bar{\sigma}_{\mathrm{e}}}{\partial\boldsymbol{b}} &= \frac{3}{4\,\bar{\sigma}_{\mathrm{e}}}\boldsymbol{\sigma} : \frac{\partial}{\partial\boldsymbol{b}^{-1}}(\mathbf{P}^{\mathrm{sym}}_{b^{-1}b^{-1},\mathrm{dev}}:\boldsymbol{\sigma}) : \frac{\partial\boldsymbol{b}^{-1}}{\partial\boldsymbol{b}}\\
\frac{\partial}{\partial\boldsymbol{b}^{-1}}(\mathbf{P}^{\mathrm{sym}}_{b^{-1}b^{-1},\mathrm{dev}}:\boldsymbol{\sigma}) &= 2\,\mathbf{P}^{\mathrm{sym}}_{Ic_2} - \frac{1}{3}((\boldsymbol{b}^{-1}:\boldsymbol{\sigma})\mathbf{I}^{\mathrm{sym}} + \boldsymbol{b}^{-1}\otimes\boldsymbol{\sigma})\\
\boldsymbol{\Phi}^*_{\beta b^m} &= \eta_1((\boldsymbol{b}^m:\boldsymbol{\beta})\mathbf{I}^{\mathrm{sym}} + \boldsymbol{b}^m\otimes\boldsymbol{\beta}) + 2\,\eta_2\mathbf{P}^{\mathrm{sym}}_{Ic_3}
\end{aligned} \tag{C3}$$

with $\boldsymbol{c}_2 \overset{\mathrm{def}}{=} \boldsymbol{b}^{-1}\cdot\boldsymbol{\sigma}$ and $\boldsymbol{c}_3 \overset{\mathrm{def}}{=} \boldsymbol{b}^m\cdot\boldsymbol{\beta}$. The derivative $\partial\boldsymbol{b}^m/\partial\boldsymbol{b}$ can be evaluated analytically, see e.g. Ekh and Runesson [15]. However, in the present implementation it is approximated by numerical differentiation.

REFERENCES

1. Lemaitre J, Chaboche J-L. *Mechanics of Solid Materials*. Cambridge, 1990.
2. Sidoroff F. Description of anisotropic damage application to elasticity. In *Physical Non-Linearities in Structural Analysis*, Hult J, Lemaitre J. (eds). IUTAM Symposium Senlis/France, Springer: Berlin, 27.-30.05, 1981.
3. Lemaitre J, Desmorat R, Sauzay M. Anisotropic damage law of evolution. *European Journal of Mechanics, Series A/Solids* 2000; **19**:187–208.
4. Chaboche J-L. Development of continuum damage mechanics for elastic solids substaining anisotropic and unilateral damage. *International Journal of Damage Mechanics* 1993; 2:311–329.
5. Dragon A, Halm D, Désoyer Th. Anisotropic damage in quasi-brittle solids: modelling, computational issues and applications. *Computational Methods and Applications in Mechanical Engineering* 2000; **183**:331–352.
6. Murakami S. Anisotropic aspects of material damage and application of continuum damage mechanics. In *Continuum Damage Mechanics*, Krajcinovic D, Lemaitre J. (eds). Number 282 in CISM Courses and Lectures, Springer: Berlin, 1987.
7. Rabier PJ. Some remarks on damage theory. *International Journal of Engineering Science* 1989; **1**:29–54.
8. He Q-C, Curnier A. A more fundamental approach to damaged elastic stress–strain relations. *International Journal of Solids and Structures* 1995; **32**(10):1433–1457.
9. Lehmann Th. Thermodynamical foundations of large inelastic deformations of solid bodies including damage. *International Journal of Plasticity* 1991; **7**:79–98.
10. Hansen NR, Schreyer HL. A thermodynamically consistent framework for theories of elastoplasticity coupled with damage. *International Journal of Solids and Structures* 1994; **31**(3):359–389.
11. Carol E, Rizzi I, Willam K. On the formulation of anisotropic elastic degradation. Part I: Theory based on a pseudo-logarithmic damage tensor rate & Part II: Generalized pseudo-Rankine model for tensile damage. *International Journal of Solids and Structures* 2001; **38**:491–518, 519–546.
12. Steinmann P, Miehe C, Stein E. Comparison of different finite deformation inelastic damage models within multiplicative plasticity for ductile materials. *International Journal of Computational Mechanics* 1993; **13**: 458–474.
13. Lämmer H, Tsakmakis Ch. Discussion of coupled elastoplasticity and damage constitutive equations for small and finite deformations. *International Journal of Plasticity* 2000; **16**:495–523.
14. Armero F, Oller S. A general framework for continuum damage models. I. Infinitesimal plastic damage models in stress space II. Integration algorithms, with applications to the numerical simulation of porous metals. *International Journal of Solids and Structures* 2000; 37(48):7409–7436, 7437–7464.
15. Ekh M, Runesson K. Bifurcation results for plasticity coupled to damage with MCR-effect. *International Journal of Solids and Structures* 2000; **37**(14):1975–1996.
16. Leckie FA, Onat ET. Tensorial nature of damage measuring internal variables. In *Physical Non-Linearities in Structural Analysis*, Hult J, Lemaitre J. (eds). IUTAM Symposium Senlis/France 1980, Springer, Berlin, 1981; 140–155.
17. Betten J. Theory of invariants in creep mechanics of anisotropic materials. In *Mechanical Behaviour of Anisotropic Materials*, Boehler JP. (ed.). EUROMECH Colloquium 115 in Grenoble 1979, Martinus Nijhoff Publishers: Dordrecht, 1982: 65–80.
18. Murakami S. Mechanical modeling of material damage. *ASME Journal of Applied Mechanics* 1988; **55**: 280–286.
19. Park T, Voyiadjis GZ. Kinematic description of damage. *ASME Journal of Applied Mechanics* 1998; **65**:93–98.
20. Steinmann P, Carol I. A framework for geometrically nonlinear continuum damage mechanics. *International Journal of Engineering Science* 1998; **36**:1793–1814.
21. Menzel A, Steinmann P. A theoretical and computational framework for anisotropic continuum damage mechanics at large strains. *International Journal of Solids and Structures* 2001; **38**:9505–9523.
22. Simo JC, Hughes TJR. *Computational Inelasticity*, In *Interdisciplinary Applied Mathematics*, vol. 7. Springer: Berlin, 1998.
23. Menzel A, Steinmann P. On the comparison of two strategies to formulate orthotropic hyper-elasticity. *Journal of Elasticity* 2001; **62**:171–201.
24. Miehe C. Numerical computation of algorithmic (consistent) tangent moduli in large-strain computational inelasticity. *Computational Methods and Applications in Mechanical Engineering* 1996; **134**:223–240.
25. Pérez-Foguet A, Rodriguez-Ferran A, Huerta A. Numerical differentiation for non-trivial consistent tangent matrices: An application to the MRS-Lade model. *International Journal for Numerical Methods in Engineering* 2000; **48**:159–184.
26. Pérez-Foguet A, Rodríguez-Ferran A, Huerta A. Numerical differentiation for local and global tangent operators in computational plasticity. *Computational Methods and Applications in Mechanical Engineering* 2000; **189**:277–296.

